Characterising the role of insulin receptors in adipogenesis

Joe Parr

Master of Science (by research) in Biomedical Science

University of York

Biology

September 2022

Abstract

Insulin possesses the ability to promote a wide range of cellular responses with links to disease states such as diabetes, cancer, and obesity. The receptors for insulin are numerous, arising from alternative splicing of the *INSR* gene and heterodimerisation of insulin receptor (IR) isoforms and insulin-like growth factor 1 receptor (IGF-1R) subunits. Whether the different cellular responses to insulin are attributable to particular receptors has not been well defined; the aim of this investigation was to elucidate this uncertainty in the context of adipogenesis. Using a human mesenchymal stem cell line (Y201 MSCs) as an alternative to the widely-used murine 3T3-L1 fibroblasts, the suitability of these cells was first determined prior to their application in the investigation of insulin signalling and adipogenesis; proteomic and functional characterisation revealed Y201 MSCs to be comparable to 3T3-L1 fibroblasts for this purpose. Analysis of the changes in expression of *INSR* and *IGF-1R* and differences in the abundance of IR:IGF-1R heterodimers provided concordant results reflecting the major roles of these proteins and revealed unexpected patterns in heterodimer formation for undifferentiated and differentiated cells following insulin stimulation. A potential explanation for these patterns was surmised but remains to be validated experimentally. Furthermore, the CRISPR-Cas9-directed generation of $INSR^{-/-}$ and $IGF\text{-}1R^{-/-}$ cell lines was performed but additional screening is required to confirm successful gene knockout. Finally, constructs enabling the expression of a double-tagged GLUT4 construct were generated to allow future analysis of the metabolic signalling capacity of each receptor. In summary, this work successfully characterised an alternative cell line with respect to adipogenesis and identified changes in IR and IGF-1R expression throughout this process; more work must be done to directly investigate the effect of each of these receptors in this process and the foundations for necessary future experimentation have been laid in this project.

List of Contents

List of tables

List of figures

Acknowledgements

I would like to thank the project supervisors and members of the Bryant and Genever lab groups for their continuous support and advice. I would additionally like to extend my deepest gratitude to Dr Dimitrios Kioumourtzoglou whose wise counsel and insight proved invaluable throughout the duration of this project.

Sincerest thanks to my parents, without whom this undertaking would not have been possible, for their unwavering moral and financial support. I am also incredibly grateful for all of the support from my partner and the encouragement of my friends in this endeavour.

Declaration

I declare that this thesis is a presentation of original work and that I am the sole author. This work has not previously been presented for an award at this, or any other, University. All sources are acknowledged as references.

Chapter 1: Introduction

1.1 Canonical insulin signalling promotes metabolic GLUT4 translocation

Physiologically speaking, insulin is best characterised for its ability to promote the postprandial clearance of circulating glucose. As an insulin secretagogue, glucose promotes the production of insulin during hyperglycaemia. The process of insulin secretion is effectuated by pancreatic beta cells where insulin is produced and stored in secretory granules prior to its release into the bloodstream (Rorsman and Renström, 2003). Circulating insulin binds to receptors on target cells which, in the context of glucose homeostasis, primarily include striated muscle cells and adipocytes (Tokarz, MacDonald and Klip, 2018). Once stimulated by insulin, these receptors initiate a signalling cascade that results in the translocation of storage vesicles to the plasma membrane (Jaldin-Fincati *et al.*, 2017). These storage vesicles harbour the protein known as glucose transporter type 4 (GLUT4) within the cell; only upon insulin stimulation do they mobilise and allow localisation of GLUT4 to the plasma membrane.

The GLUT family comprises three separate classes encompassing 14 different proteins expressed in humans (Mueckler and Thorens, 2013). All of these proteins are similar in terms of structure, with each exhibiting 12 transmembrane domains among other similarities, but each displays variable specificity for substrates (primarily hexoses and polyols) and differ with regard to tissue-specific distribution (Mueckler and Thorens, 2013). Due to the necessity of GLUT4 in the metabolic response to insulin, the protein is predominantly expressed in the striated muscle and adipose tissue targeted by insulin (Charron *et al.*, 1989; Tokarz, MacDonald and Klip, 2018). Upon translocation, GLUT4 acts as a facilitative glucose transporter, enabling the flux of glucose from the blood into the cell. This serves to lower the concentration of circulating glucose that initially stimulated insulin production. In the absence of an insulin stimulus, surface-localised GLUT4 undergoes retrograde transport via clathrin-mediated endocytosis, causing the protein to be sequestered once again in intracellular vesicles (Shigematsu *et al.*, 2003).

1.2 Insulin receptor complexity arises from alternative splicing and heterodimerisation

Although insulin is associated with regulating the metabolic function of adipocytes and muscle cells, receptors for insulin are thought to be expressed ubiquitously such as in bone, brain, and reproductive tissues (Havrankova, Roth and Brownstein, 1978; Fulzele *et al.*, 2010; Wu *et al.*, 2012). One potential explanation for this widespread distribution is that there are several insulin receptors (IRs) that all bind insulin at varying degrees of affinity. The insulin receptor gene, *INSR*, undergoes alternative splicing during transcription to

generate two isoforms, insulin receptor A, IR-A, and insulin receptor B, IR-B. At an elementary level, these isoforms each consist of two subunits, denoted α and β, linked by disulphide bonds (αβ) (Kasuga *et al.*, 1982). These two isoforms are monomers and can each homodimerise $(\alpha\beta)_2$ to form two distinct receptors, also referred to as IR-A and IR-B. Moreover, these monomers can heterodimerise to form a hybrid IR-A:IR-B receptor. To further complicate the situation, insulin also binds, with low affinity, to the insulin-like growth factor 1 receptor (IGF-1R) which shares many structural and functional similarities with IRs, including its dimeric nature. Consequently, IGF-1R monomers display promiscuity with IR isoforms leading to the generation of IGF-1R:IR-A, and IGF-1R:IR-B heterodimeric receptors. This gives a total of six insulin-binding receptors (Fig. 1) that can all be present on a single cell in varying proportions (Bailyes *et al.*, 1997).

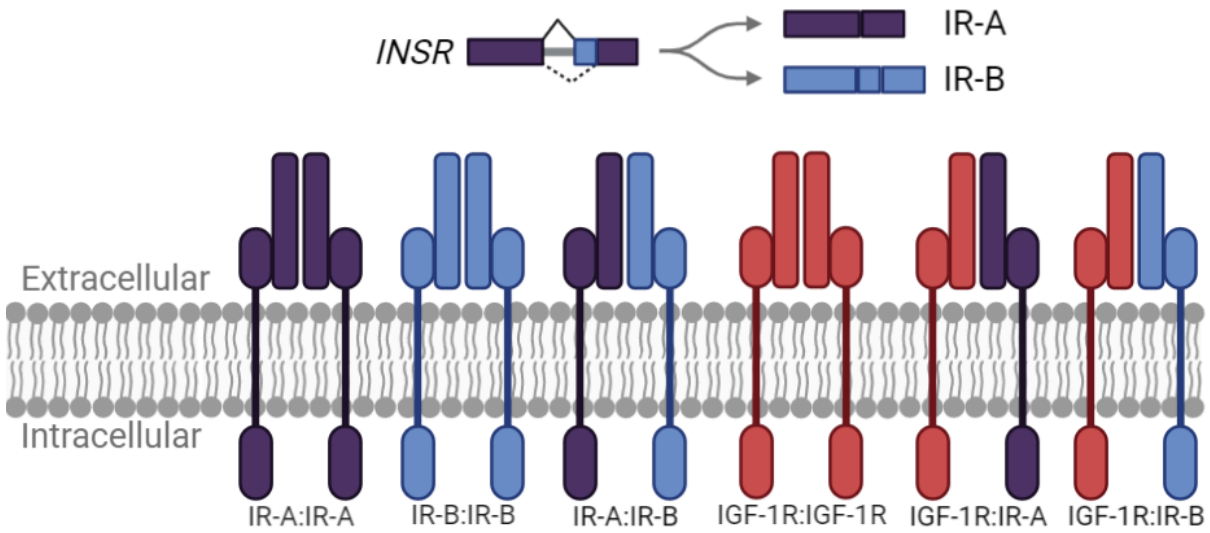

Figure 1: Composition and provenance of major insulin receptors. The six major insulin-binding receptors arising as a result of alternative splicing and hybridisation between IR and IGF-1R subunits. Created with BioRender.

Biochemically, all of these receptors are receptor tyrosine kinases (RTKs), with several noteworthy functional domains. The α subunits of the monomeric IR isoforms (Fig. 2) are entirely extracellular, each with two N-terminal leucine-rich repeat domains (L1 and L2) either side of a cysteine-rich domain (CR), followed by three fibronectin type III domains (FnIII-1, FnIII-2, and FnIII-3) at the C-terminus. The L1 region of the α subunit facilitates insulin binding (Smith *et al.*, 2010) but, in the case of IR-B, may be influenced by the peptide sequence encoded by exon 11, included in this isoform as a result of alternative splicing. The presence of this peptide sequence in the IR-B ectodomain modulates its ability to bind ligands, namely insulin and IGF-2, which both bind to the exon 11^- IR-A ectodomain with a higher affinity (Mosthaf *et al.*, 1990; Frasca *et al.*, 1999). Disulphide bonds link the C-terminal region of the α subunit with the extracellular N-terminal domain of the β subunit (Cheatham and Kahn, 1992). The β subunit possesses the eponymous tyrosine kinase

domain, essential for the transduction of insulin signalling. Following receptor stimulation, the tyrosine kinase domains on each β subunit of the dimeric receptor mediate transphosphorylation of the Tyr-1146 and Tyr-1150/1151 residues of their partner, leading to a cascade of tyrosine phosphorylation (White *et al.*, 1988). These phosphotyrosine residues act as loci for the recruitment of adaptor proteins such as SHC-transforming protein 1 (SHC1) and insulin receptor substrate 1 (IRS-1) which serve as signalling platforms for the pathways downstream of insulin receptors (Sun *et al.*, 1991; Gustafson *et al.*, 1995), the most notable of which is arguably the PI3K/Akt pathway (Shepherd, Withers and Siddle, 1998). Despite this well-characterised tyrosine kinase mechanism, recent research suggests that IR and IGF-1R can also act as nuclear receptors, translocating to the nucleus and binding to specific genomic sequences (Werner, Sarfstein and Laron, 2021). Clearly, not all mechanisms of insulin signalling have been fully characterised, which demonstrates the need for further understanding of the signalling pathways emanating from insulin receptors.

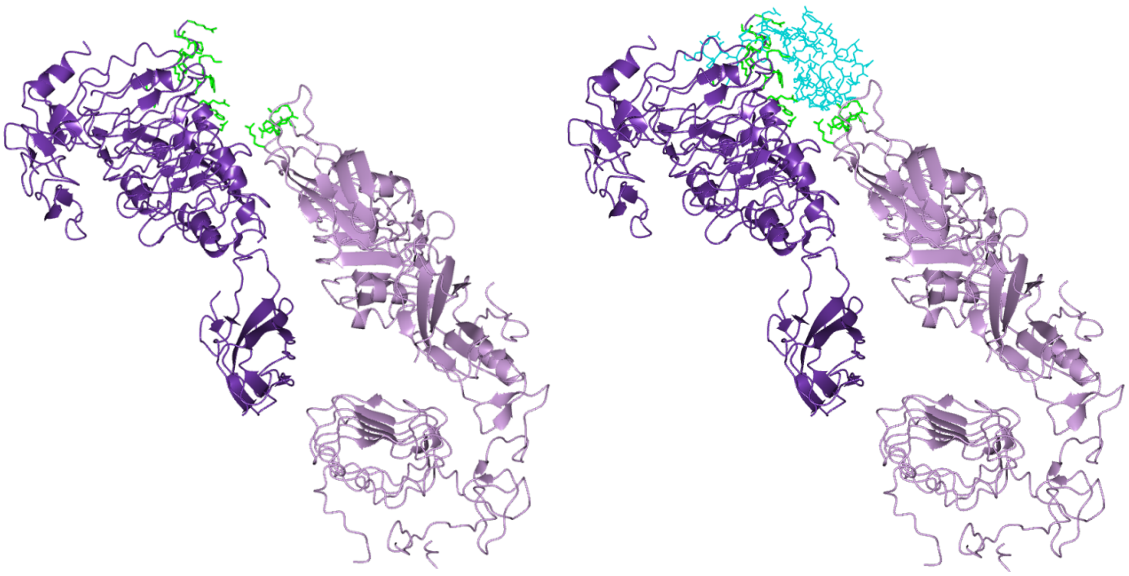

Figure 2: Ectodomain structure of a homodimeric insulin-bound IR. Separate alpha subunits are shown in purple and lilac, insulin-binding regions are shown in green, insulin is shown in cyan. Beta subunits are not shown. Protein structure obtained from the Protein Data Bank in Europe (PDBe), PDB ID: 6ce7 (Scapin *et al.*, 2018).

1.3 Diabetes mellitus has a significant global disease burden

Due to its links to glucose homeostasis, insulin is often associated with the development and management of diabetes. The term diabetes mellitus encompasses two distinct metabolic disorders; type I diabetes mellitus (T1DM), characterised by the autoimmune destruction of pancreatic beta cells responsible for insulin production, and type II diabetes mellitus (T2DM), arising from the failure of target cells to respond to insulin signalling. Diabetes mellitus has a significant global disease burden and T2DM accounts for 95% of all

cases (World Health Organization, 2021a). With an estimated 422 million people suffering from diabetes mellitus in 2014 and a death toll of 1.5 million in 2019 (World Health Organization, 2021a), the prevalence of this metabolic disease is increasing at an alarming rate (Fig. 3); 79 million DALYs are predicted to be lost in 2025 alone (Lin *et al.*, 2020). Modern studies have identified several heritable elements such as SNPs that underpin the multifactorial development of T2DM (Salanti *et al.*, 2009; Ali, 2013) but this does not take into consideration the environmental factors that play an equally pivotal role. The frequent concomitance of T2DM with obesity (Verma and Hussain, 2017) lends credence to the concept that poor diet and physical inactivity are major drivers of T2DM development (Orozco *et al.*, 2008), with obesity acting as a significant risk factor (Hillier and Pedula, 2003).

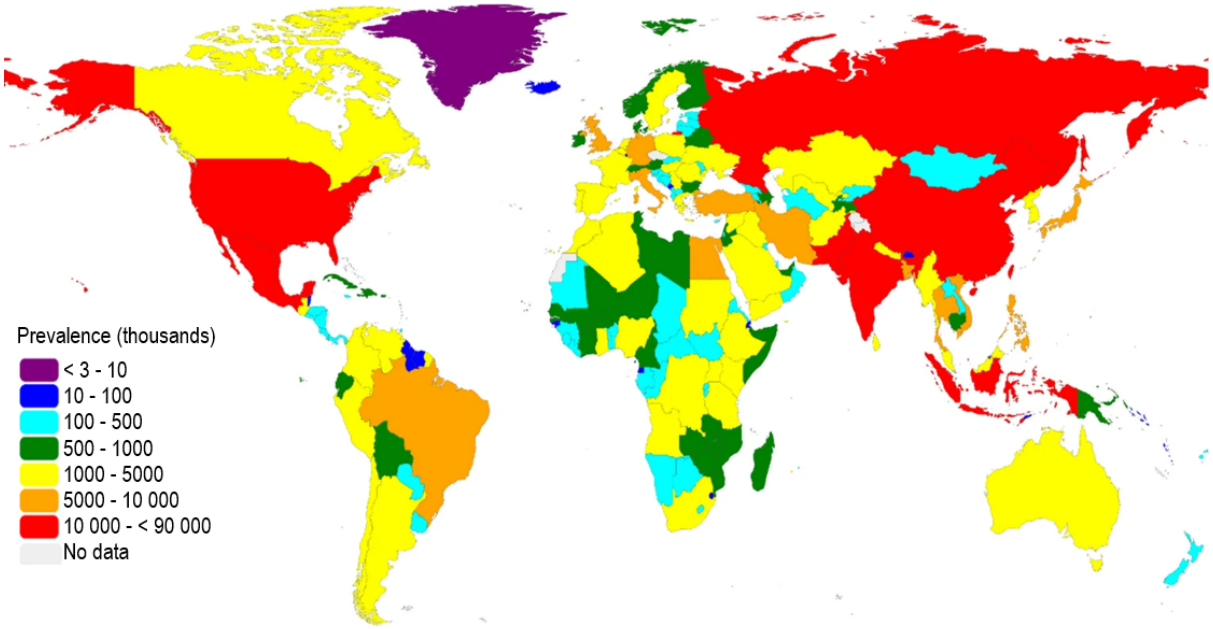

Figure 3: The global prevalence of diabetes in 2017. Adapted from (Lin *et al.*, 2020).

With the consumption of a high-glucose diet, insulin production increases accordingly (Castell-Auví *et al.*, 2012). This pre-diabetic hyperinsulinemia is strongly correlated with the development of insulin resistance (Kim and Reaven, 2008; Silbernagel *et al.*, 2011) but the signalling events and mechanisms involved in this process are poorly understood. Once early insulin resistance emerges, glucose homeostasis becomes dysregulated and compensatory hyperinsulinemia arises (Dubuc, 1976) with the potential to progress to T2DM. The development of T2DM can cause a range of life-changing symptoms and complications such as blindness, stroke, and peripheral artery disease leading to lower extremity amputation (Jørgensen *et al.*, 1994; Trautner *et al.*, 1997; Barnes *et al.*, 2020; Khan *et al.*, 2021). One of the most noteworthy complications, however, is the development of several types of cancer, including pancreatic, colorectal, and ovarian cancers (Larsson, Orsini and Wolk, 2005; Wang *et al.*, 2017; A. M. Y. Zhang *et al.*, 2019). This is likely due to

the ubiquitous mitogenic activity exhibited by insulin upon reaching a hyperinsulinemic state (Pisani, 2008; Kilvert and Fox, 2020) combined with the fact that insulin receptors are overexpressed in some types of cancer (Papa *et al.*, 1990). It has also been suggested that obesity, already comorbid with diabetes, acts as a major risk factor for the development of cancers associated with insulin signalling (Morrione and Belfiore, 2022), strengthening the link between these three diseases. Some drugs used for the management of diabetes, such as certain sulphonylureas, can further exacerbate the risk of cancer (Monami *et al.*, 2009), and others used to treat insulin-associated cancers can cause hyperinsulinaemia and increase the risk of diabetes (Haluska *et al.*, 2006). This overlap makes diabetes and its complications difficult to treat; it is crucial that the signalling pathways and receptors involved in these events are better understood for the development of safe and efficacious therapeutic interventions.

1.4 Insulin signalling is implicated in the development of several cancers

Partly due to the number of receptors with a potential involvement in signal transduction, insulin stimulation activates signalling through a complex network of interwoven pathways (Fig. 4) responsible for the regulation of many crucial cellular processes (Krüger *et al.*, 2008). The most notable and well-defined of these responses is the metabolic GLUT4 translocation central to the regulation of whole-body glucose homeostasis. However, one effect of insulin signalling is of particular interest to modern biomedical research; the signalling network activated by insulin includes the Ras/MAPK pathway (Goalstone *et al.*, 1997; Xu *et al.*, 2006) which lends insulin the ability to act as a potent mitogenic growth factor in addition to its characteristic role in metabolism. Activation of the Ras/MAPK pathway in this manner allows insulin to promote the development of cancer (Wang *et al.*, 2012), which has been confirmed in several instances with regard to insulin receptor signalling (Giorgino *et al.*, 1991; Rose *et al.*, 2007). Experimentally, a correlation between insulin levels and the incidence of cancer has been observed on many occasions across multiple models with a variety of methodological approaches (Heuson and Legros, 1972; Tran, Medline and Bruce, 1996; Kabat *et al.*, 2009). This further highlights the clinical importance of understanding the cellular response to insulin.

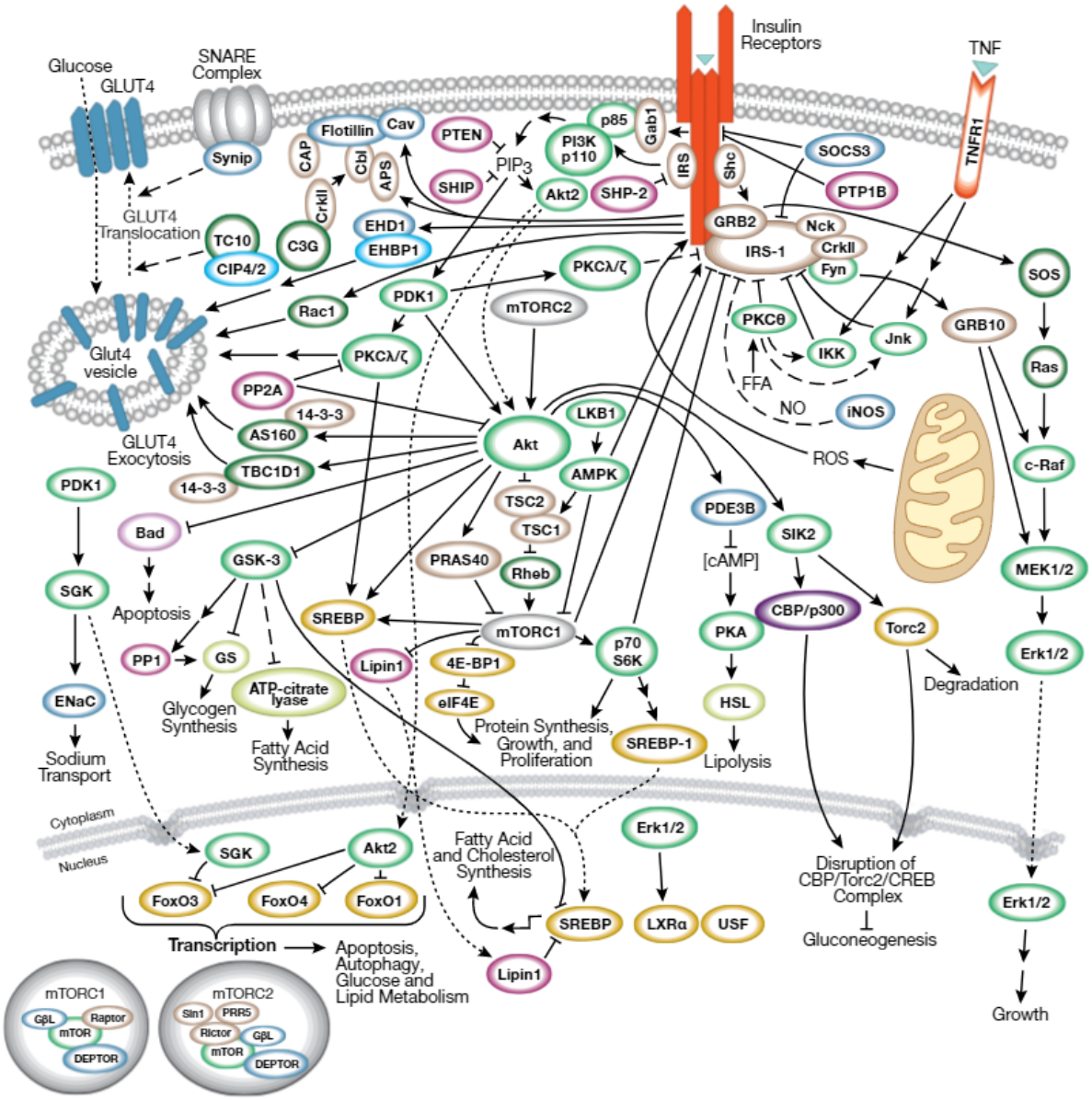

Figure 4: Insulin receptor signalling and crosstalk. The signalling pathways and cellular responses activated as a result of insulin receptor stimulation (Cell Signaling Technology, 2003). Of note are the Ras/MAPK pathway leading to cell growth, and the PI3K/Akt pathway leading to GLUT4 translocation. Ellipses denote individual proteins with colours corresponding to protein classes: purple = acetylase, beige = adaptor, pale pink = regulator of autophagy/apoptosis, bright blue = deacetylase/cytoskeletal protein, dark green = GTPase/GAP/GEF, light green = kinase, pale green = metabolic enzyme, magenta = phosphatase, grey = protein complex, yellow = transcription/translation factor, orange = receptor, pale blue = other. Solid lines indicate direct processes, dashed lines indicate tentative processes, and dotted lines indicate translocation. Pointed arrowheads show stimulatory modification, flat arrowheads show inhibitory modification, and bent lines show transcriptional modification.

The ratio of receptors on a target cell is thought to be a major deciding factor in each cellular response generated by insulin stimulation and the temporally-regulated preferential alternative splicing of the *INSR* gene may reflect this (Savkur, Philips and Cooper, 2001;

Serrano *et al.*, 2005). While it is apparent from related literature that the response to insulin depends somewhat on the proportion of each receptor expressed on the cell, this is not a strict correlation as receptor responses have been shown to vary with differences in factors such as ligand binding affinity and kinetics, and downstream receptor substrate recruitment (Hansen *et al.*, 1996; Morcavallo *et al.*, 2011). This may explain how different ligands for a single insulin-binding receptor could elicit different cellular responses, but how insulin itself can differentially activate the metabolic or mitogenic pathways is not entirely understood. Although It has been shown that the insulin-stimulated mitogenic Ras/MAPK and metabolic PI3K pathways can be independently modulated with no change in total IR expression, changes in the proportion of each receptor isoform have not been characterised in this context (Cusi *et al.*, 2000). These observations highlight a need for further investigation into the activity of each receptor to determine their individual involvement with the insulin-stimulated pathways that generate a variety of cellular outputs.

Table 1: The ligand-binding affinities of homodimeric insulin receptors. Reported EC_{50} values (nM) of insulin, IGF-1, and IGF-2 for homodimeric receptors. Repeated references denote the use of multiple methods to determine EC_{50} values. EC_{50} = concentration of insulin required to achieve 50% of maximal receptor activation. *ND* = not determined. Adapted from (Belfiore *et al.*, 2017).

Ligand	IR-A	IR-B	IGF-1R	Reference
Insulin	0.91 ± 0.3	1.0 ± 0.4	*ND*	(Frasca *et al.*, 1999)
	ND	*ND*	> 30	(Pandini *et al.*, 2002)
	0.40 ± 0.10	0.49 ± 0.05	> 1000	(Sciacca *et al.*, 2010)
	ND	*ND*	383 ± 27	(Versteyhe *et al.*, 2013)
	1.57 ± 0.33	*ND*	*ND*	(Rajapaksha and Forbes, 2015)
	2.7 ± 0.6	2.6 ± 0.7	*ND*	(Pierre-Eugene *et al.*, 2012)
IGF-1	> 30	> 30	0.2 ± 0.3	(Pandini *et al.*, 2002)
	ND	*ND*	1.49 ± 0.14	(Versteyhe *et al.*, 2013)
	34 ± 13	50 ± 13	*ND*	(Pierre-Eugene *et al.*, 2012)
IGF-2	3.3 ± 0.4	36.0 ± 3.8	*ND*	(Frasca *et al.*, 1999)
	ND	*ND*	0.6	(Pandini *et al.*, 2002)
	ND	*ND*	13.1 ± 0.7	(Versteyhe *et al.*, 2013)
	15.2 ± 0.2	*ND*	*ND*	(Rajapaksha and Forbes, 2015)
	4 ± 0.4	*ND*	3.4 ± 0.2	(Ziegler *et al.*, 2014)

1.5 Obesity expedites the development of diabetes

Similarly to the global pandemic of T2DM, the prevalence of obesity is also increasing exponentially worldwide; 8.5% of the Earth's population were classed as obese in 2016 (World Health Organization, 2021b), with this figure predicted to surpass 13% by 2030 (Lobstein, Brinsden and Neveux, 2022). Like T2DM, the risk factors for obesity are numerous, with poor diet and physical inactivity having a significant impact on its development. Several confounding factors link obesity to the development of insulin resistance and T2DM; adipocytes, which make up a large proportion of adipose tissue and provide lipid storage, can regulate metabolism with the secretion of hormones, non-esterified fatty acids (NEFAs), and adipokines that can all contribute to inflammation and reduced sensitivity of adipocytes to insulin (Groop *et al.*, 1991; Lord, 2006; Scherer, 2006; Johnston *et al.*, 2018). NEFAs are also observed at an increased level in T2DM and are shown to reduce insulin sensitivity by inhibiting GLUT4 expression leading to reduced glucose transport (Roden *et al.*, 1996) as well as being linked to impaired insulin production and secretion (Zhou and Grill, 1994). It is through these mechanisms, among others, that the high levels of adipose tissue characteristic of obesity are able to promote the development of insulin resistance and T2DM. This could implicate insulin signalling in a cycle whereby high blood glucose levels from factors such as poor diet promote insulin secretion which in turn promotes the formation of adipose tissue resulting in insulin resistance via NEFA production, causing overcompensation in insulin production and eventually resulting in T2DM and its complications. What further complicates this situation is that insulin signalling is critical in adipogenesis, the formation of adipose tissue.

1.6 Insulin is a major driver of adipogenesis

The term MSC refers to mesenchymal stem cells, a self-renewing multipotent population of cells first isolated from bone marrow (Friedenstein, Chailakhjan and Lalykina, 1970), but present throughout various tissues and fluids such as adipose tissue, dental pulp, and menstrual blood (Zuk *et al.*, 2001; Patel *et al.*, 2008; Agha-Hosseini *et al.*, 2010). Three major pathways by which MSCs can differentiate are the osteogenic, chondrogenic, and adipogenic lineages (Ullah, Subbarao and Rho, 2015). Adipogenesis describes the differentiation and maturation of adipocytes from these MSCs, which can be observed proteomically, based on changes in cellular markers of adipocytes, and visually, through changes in cell morphology such as accumulation of lipid droplets. During adipogenesis, MSCs pass through a number of intermediate stages, such as committed preadipocytes, prior to terminal differentiation and maturation (Lefterova and Lazar, 2009). The pathways regulating this process are still under active investigation, especially with regard to MSC origin and adipocyte lineage commitment (Ali *et al.*, 2013); adipogenesis is a process regulated by many cell signalling events, including peroxisome proliferator-activated

receptor gamma (PPAR-γ) and C/EBPα interaction (Rosen *et al.*, 2002) as well as Wnt/β-catenin signalling (Prestwich and Macdougald, 2007). In addition to these is IR signalling, a known driver of adipogenesis due to the reduced ability of $IR^{-/-}$ cells to differentiate into adipocytes (Gupta *et al.*, 2018). The insulin signalling pathway has been shown to activate lipogenesis and inhibit lipolysis through a range of intermediate proteins including sterol regulatory element-binding transcription factor 1c (SREBP-1c) and mammalian target of rapamycin complex 1 (mTORC1) (Foretz *et al.*, 1999; Dif *et al.*, 2006; Chakrabarti *et al.*, 2013); the specific insulin receptors involved with signal transduction through these proteins have not yet been characterised.

1.7 Modulation of Insulin signalling could influence MSC differentiation

Regenerative medicine is a modern field of clinical research that aims to treat a range of diseases and symptoms of ageing by providing the patient's body with the factors necessary to promote tissue regeneration *in situ*. These therapies can take many forms including the development of transplantable grafts and bioactive scaffolds, organoid culture, and direct inoculation of autologous or allogeneic cells (Hoexter, 2002; Carr *et al.*, 2008; Rodríguez-Vázquez *et al.*, 2015; Okamoto *et al.*, 2020). The therapeutic potential of modern regenerative medicine is very promising but difficulties with clinical translation and standardisation of cellular products hinder advancement in this field (Cao *et al.*, 2021). One target of regenerative medicine under particularly active investigation is osteoarthritis. Current research aims to ameliorate the cause and symptoms of this condition by promoting the regeneration of cartilage in joints such as the knee, with MSCs being the forerunner for this type of therapy (Murphy *et al.*, 2003). MSCs are attractive with regard to osteoarthritis due to their chondrogenic potential; the idea that these cells can differentiate into cartilage to regenerate meniscal tissue makes them an obvious choice for the treatment of osteoarthritis. However, due to factors such as the low engraftment rate of injected MSCs observed across many studies (Prockop, 2007), it is thought to be rather a result of paracrine signalling that these cells can promote regeneration in this context (Murphy, Moncivais and Caplan, 2013).

One of the major issues with MSC therapies is the natural heterogeneity of this cell population; sorted MSC populations can still exhibit heterogeneity (Kolf, Cho and Tuan, 2007), a property that can result in deleterious complications such as thromboembolism (Tatsumi *et al.*, 2013). Furthermore, it is apparent that MSCs obtained from different sources and cultured *in vitro* under different conditions exhibit variability with regard to functional characteristics and clinical potential (Costa *et al.*, 2021). These heterogeneity-induced difficulties draw attention to the need for standardisation of cellular products such as MSC therapies, a process that could be aided by drawing upon knowledge of insulin signalling. As discussed, insulin signalling plays a pivotal role in the differentiation of MSCs into adipocytes but insulin has also been seen to influence

chondrogenesis and osteogenesis (Phornphutkul, Wu and Gruppuso, 2006; Ferron *et al.*, 2010; Zhang *et al.*, 2020), two processes that can be utilised for MSC regenerative therapies. Which insulin-binding receptors are involved in these processes has not currently been defined. If separate receptors are involved in each differentiation scheme, it may be possible to enhance adipogenesis, osteogenesis, or chondrogenesis in a clinical setting by inhibiting the other signalling pathways associated with the receptors, thereby reducing heterogeneity in the context of differentiation.

1.8 Project aims

It is clear from the literature that much remains to be elucidated with regard to the role of IRs and IGF-1R in the various cellular responses to insulin. This project aims to explore several receptors for insulin on an independent basis to determine to what extent they are associated with some of the cellular processes that emanate from insulin stimulation. The main focus of this investigation will be on adipogenesis, with the objective to determine the capacity of IR, IGF-1R, and IR:IGF-1R hybrids to support this process and identify whether any particular receptors have a more significant involvement in promoting adipocyte differentiation than others. T2DM and insulin-associated cancers, and their link to adipogenesis and obesity, will be taken into account but not experimentally evaluated in this investigation in order to pave the way for future work that may look to further explore these disease states. Additionally, while IR-A and IR-B will not be independently analysed, rather these will both fall under the term IR in the present investigation, these isoforms will be considered for the interpretation of results and will be separated for experimental analysis in future work.

To make this investigation physiologically relevant with regard to the aforementioned disease states, a hTERT-immortalised human mesenchymal stem cell line (James *et al.*, 2015) (herein referred to as Y201 MSCs) will be employed as these cells can be differentiated into the adipocytes necessary for this work and provide an accurate model upon which to base investigations into human diseases. Expanding on the idea of appropriate models in the context of T2DM, many modern investigations have used induced-diabetic rodent models to analyse T2DM and its effects which may not be as accurate when extending findings to a clinical setting. The reason for this is due to a number of SNPs in the regulatory mechanisms for insulin signalling that are thought to underpin the development of human T2DM (Staiger *et al.*, 2009). While some of the pathophysiological effects of this disease can be individually replicated with rodent models, it may be difficult to generate a completely analogous model of human T2DM (Kottaisamy *et al.*, 2021), especially on a cellular level; rodents are unlikely to provide an accurate platform for analysis of the complexities observed with human T2DM. The use of Y201 MSCs in the present investigation aims to bypass this shortcoming, using a novel approach

to achieve results with more relevance with regard to the cellular mechanisms of human insulin signalling.

These cells' suitability will be validated prior to their use as a foundation for the creation of two cell knockouts, meaning two cell lines will be generated to express either IR or IGF-1R in isolation. The stimulation of adipogenesis in each of these cell lines will permit analysis of the capacity of each receptor to facilitate the differentiation and maturation of adipocytes on an independent level, evaluated based on adipocyte marker expression and lipid droplet accumulation. Additionally, the proportion of the IR:IGF-1R hybrid receptor will be quantified before and after adipogenesis, which may shed light on the role of receptor hybrids during the differentiation process. This investigation aims to obtain novel insights into the function of several receptors on an individual basis with regard to adipogenesis, feeding into the overall aim of delineating the complex interwoven pathways associated with insulin signalling that allow this protein to elicit distinct cellular responses.

Chapter 2: Materials and methods

2.1 Cell culture methods

2.1.1 Y201 MSC cell culture

hTERT-immortalised human bone-marrow-derived mesenchymal stem cells (BMSCs) (James *et al.*, 2015), referred to herein as Y201 MSCs, were employed in this investigation as a foundation for all cell-based analyses. Cell culture medium was prepared with Dulbecco's Modified Eagle Medium (DMEM) (Gibco; 21969-315) supplemented with Glutamax (Gibco; 35050-061), 1% (v/v) penicillin/streptomycin, and 10% (v/v) FBS. This solution was passed through a 0.22μm filter for sterility prior to use. Cell cultures were incubated at 37°C, 5% CO_2.

2.1.2 Induction of adipogenesis

For the induction of adipogenesis, confluent Y201 MSCs were cultured in adipogenic medium comprising: 1μM human insulin, 100μM indomethacin, 1μM dexamethasone, and 500μM 3-isobutyl-1-methylxanthine (IBMX), as described by Pittenger et al. (Pittenger *et al.*, 1999). Differentiating cell cultures were incubated at 37°C, 5% CO_2. Medium was changed twice weekly for 21 days before analysis of adipogenic differentiation was conducted.

2.1.3 Preparation of whole-cell lysates

Confluent Y201 MSCs and Y201-derived adipocytes at various stages of differentiation were kept on ice throughout this procedure. These cell cultures were washed three times with ice-cold PBS before being scraped in the presence of 50ul (per well of a 6-well culture plate) cold lysis buffer comprising 50mM HEPES solution, 150mM NaCl, 5mM EDTA, 1% v/v Triton X-100 and 1 EDTA-free protease inhibitor tablet (Roche; 05892791001) in a total volume of 10ml. Scraped cells were homogenised by pulling samples through a 25G needle ten times before pulling through a 26G needle twice. Samples were centrifuged at 500g for 10 minutes at 4°C before discarding the pellet and adipocyte lipid layer and rotating on a wheel at 4°C for 60 minutes. Samples were then centrifuged at 13000 rpm for 15 minutes at 4°C and pellets were discarded. An equal volume of 2x Laemmli Sample Buffer + 10% v/v β-mercaptoethanol was added to each sample which were then heated at 65°C for 10 minutes. For lysis of Y201 MSCs, the 500g centrifugation and 60 minute rotation steps were omitted. These whole-cell lysates were stored at -20°C until analysis via SDS-PAGE.

2.1.4 Oil red O staining

Oil red O (ORO) staining was used to visualise lipid droplet accumulation at time points during adipogenesis. Y201 MSCs were plated at weekly intervals in a single row of the same 24-well plate and stimulated to undergo adipogenesis as in section 2.1.2 four days after plating to allow the cells to reach 100% confluence. This was performed for three weeks such that on day 21 of differentiating the first group of MSCs, four groups of cells at stages of differentiation from 0 days to 21 days were ready for staining. For preparation of a stock solution of oil red O, 0.5g oil red O was dissolved in 100ml of isopropanol which was passed through a 0.22µm filter after incubation for one hour. The oil red O working solution was prepared by mixing 6ml stock with 4ml ddH_2O and incubating for one hour before filtering once again through a 0.22µm filter. This working solution was used within 3 hours of preparation to ensure stability of the stain. Prior to ORO staining, all Y201 MSC and adipocyte cultures were washed twice with PBS before fixing with 500µl per well of 4% paraformaldehyde (PFA) for 10 minutes at 37°C. PFA was removed and samples were washed once with ddH_2O before adding 500µl per well of 60% isopropanol and incubating at 37°C for 5 minutes. Isopropanol was discarded and 250µl of oil red O working solution was added to each well and incubated once again at 37°C for 10 minutes. After removal of the stain, samples were washed once with 60% isopropanol before three washes with ddH_2O. Stained samples were then imaged using visible light microscopy.

2.1.5 Generation of *INSR* and *IGF-1R* knockout cells

Y201 MSC cultures underwent knockout of either *INSR* or *IGF-1R* using Xfect Transfection Reagent (Takara Bio; 631318) to transfect either an *INSR*-targeted or *IGF-1R*-targeted RFP-expressing CRISPR-Cas9 construct (targeting AACTGCCCGTTGATGACGG or ATGATGCGATTCTTCGACG for *INSR* and *IGF-1R* respectively). Expression of this construct was observed via RFP fluorescence. These cells underwent sorting and expansion to obtain clonal populations.

2.1.6 Clonal expansion of knockout candidates

Following transfection of the RFP-tagged Cas9 constructs, the Y201 MSCs were sorted using FACS to isolate cells expressing high levels of RFP. For each plasmid transfected, 96 fluorescent cells were individually sorted into a 96-well plate and cells were also sorted in rows of 5, 10, 20, and 50 cells per well in a 24-well plate, using conditioned cell culture medium supplemented with 20% HyClone FBS in all plates. Colonies were isolated from the 96 well plates for clonal expansion and LN_2 storage in FBS supplemented with 10% DMSO as candidate *INSR* or *IGF-1R* knockouts awaiting screening. Heterogeneous cell populations were isolated from the 24-well plate and expanded prior to serial dilution for the

acquisition of clonal populations. These populations were expanded and moved to LN_2 storage as before prior to confirmation of *INSR* or *IGF-1R* knockout. Due to issues with cell viability post-transfection, many candidates were lost throughout the expansion process and additional Y201 *INSR* and *IGF-1R* knockout candidates, generated in previous work, were provided by D. Kioumourtzoglou to increase the likelihood of success. Knockout candidates were screened via SDS-PAGE and Western blotting for IR or IGF-1R as in section 2.2.3. Absence of bands at ~95kDa was suggestive of successful knockout for either receptor.

2.1.7 Insulin stimulation of Y201 MSCs and Y201-derived adipocytes

Y201 MSC and Y201-derived adipocyte cell cultures were serum starved for 2 hours prior to insulin stimulation for cell cycle synchronisation. These cell cultures were exposed to 12μM human insulin in serum free medium for various lengths of time prior to analysis via PLA.

2.1.8 Proximity ligation assay (PLA)

To generate adipocyte cultures for PLA, Y201 cells were plated in two 8-chambered slides (ThermoScientific; 154534) and cultured until complete confluence. These cultures then underwent adipogenesis as in section 2.1.2. At day 17 of differentiation, an additional 8-chambered slide was prepared with Y201 cells to provide a confluent population of MSCs for PLA by day 21. On day 21, all cell cultures underwent insulin stimulation as in section 2.1.7 for 0 minutes, 5 minutes, 10 minutes, or 20 minutes. The adipocyte-containing slide and MSC-containing slide (denoted by A and B respectively) had this stimulation performed in duplicate; the second adipocyte-containing slide, to be used as a control group (denoted by C), underwent only 0 minutes and 10 minutes of stimulation in duplicate. Cells were washed twice with PBS before fixing with 200μl per well of 3% PFA for 30 minutes at room temperature. PFA was quenched by two washes of 400μl 20mM glycine in PBS. For blocking and permeabilisation of the cells, 200μl of BSA/GLY/SAP (comprising 0.1% w/v saponin, 2% w/v BSA, and 20mM glycine in PBS) was added to each chamber before 30 minute incubation at 37°C. The primary antibodies used for this PLA were as follows: α-IRβ mAb (Abcam; ab69508), and α-IGF-1Rβ mAb (Cell Signalling Technology; 3018). These antibodies were diluted 1:100 in BSA/GLY/SAP and 100μl of combined antibody solution (1:1 mixture of both diluted antibodies) was added to all chambers on slides A and B. Diluted antibodies were added individually to the control chambers on slide C to confirm negative PLA signal in the absence of both antibodies. Primary antibody incubations were performed at 37°C overnight.

The following day, chamber walls were removed from each slide before washing slides in room temperature BSA/GLY/SAP for 10 minutes with orbital shaking. After washing, slides were dried with gentle aspiration around the borders of each former chamber to allow the formation of open droplet reactions in the next step. PLA probes were diluted 1:5 in BSA/GLY/SAP before adding 40µl to each cell-containing region of each slide and incubating at 37°C for one hour. The PLA probe solution was tapped off before washing each slide twice in wash buffer A (Sigma Aldrich; DUO82046) for 5 minutes each with orbital shaking. Ligase buffer was diluted 1:5 on ice in ddH_2O, taking addition of the ligase into account when calculating the final volume to allow 1:40 dilution of the ligase on ice. 40µl of this ligase solution was added to each sample prior to incubation at 37°C for 30 minutes. Ligation solution was tapped off before washing each slide twice in wash buffer A for 2 minutes with orbital shaking; wash buffer was then tapped off and gently aspirated from each slide. Amplification buffer was diluted 1:5 in ddH_2O before addition of polymerase 1:80 immediately before addition of 40µl of this solution to each of the samples and incubation at 37°C for 100 minutes. From this point, all steps were performed in the dark where possible. Polymerase solution was tapped off before washing each slide twice in wash buffer B (Sigma Aldrich; DUO82048) for 10 minutes each with orbital shaking before washing once more in 0.01X wash buffer B for 1 minute. Excess wash buffer was gently aspirated before allowing each slide to air-dry completely at room temperature. Once dry, cover slips were placed on each slide using Duolink In Situ Mounting Medium with DAPI, all edges of the cover slip were then sealed using nail polish. The nail polish was allowed to dry for 15 minutes before checking each slide in a fluorescence microscope. Slides were stored at -20°C before analysis using a Zeiss LSM 880 confocal microscope with Airyscan.

2.2 Molecular biology methods

2.2.1 Creation of a double-tagged GLUT4 construct

To generate the plasmids required for the replacement of endogenous GLUT4 with the double-tagged construct, pSpCas9n(BB)-2A-Puro (PX462) V2.0 (Addgene plasmid # 62987) (Ran *et al.*, 2013) was used as a vector for the cloning of GLUT4 5' and 3' homology arms individually, as described by Ran et al. (Ran *et al.*, 2013). Successful recombination was identified via BbsI diagnostic digest and confirmed via Sanger sequencing (Eurofins Genomics). The double-tagged GLUT4 construct to be inserted into the genomic GLUT4 locus was linearised via partial PCR amplification of the parental plasmid followed by DpnI digestion for removal of circular DNA.

2.2.2 Plasmid extraction

Plasmids were extracted from 10ml overnight cultures using Wizard® Plus SV Minipreps DNA Purification Systems (Promega; A1460) following the spin format protocol. Plasmids were extracted from 50ml overnight cultures using a HiSpeed Plasmid Midi Kit (Qiagen; 12643).

2.2.3 SDS-PAGE and Western blotting

For analysis of Y201 MSC and adipocyte protein content, including adipocyte markers and IRs/IGF-1R, whole-cell lysates from undifferentiated MSCs and from adipocytes at various stages of differentiation underwent separation via SDS-PAGE, using 12% polyacrylamide gels in all cases except IR and IGF-1R for which 7.5% polyacrylamide gels were used. Precision Plus Protein™ All Blue Prestained Protein Standards enabled identification of protein bands (Bio-Rad; 1610373). Electrophoresis was performed at 100V for around 90 minutes for all gels. Proteins were transferred to nitrocellulose membranes at 0.35A for 60 minutes prior to membrane blocking, performed using a 5% BSA solution in TBST for 75 minutes. This was followed by membrane cutting and overnight incubation of each membrane section at 4°C with the corresponding specific primary antibody (Table 2). After pouring off the primary antibody, membranes were washed three times for 10 minutes each with TBST before the addition of secondary antibodies. Secondary antibody incubations were performed for 2 hours at room temperature prior to pouring off and repeating the TBST washes as before. Membranes were visualised using SuperSignal™ West Pico PLUS Chemiluminescent Substrate (ThermoScientific; 34577) with the iBright Imaging System (Invitrogen).

Table 2: Antibodies used for western blot analysis.

Protein	Primary antibody	Species	Secondary antibody
FABP4	α-FABP4 antibody (Abcam; ab23693)	Rabbit	α-rabbit HRP-linked IgG, (Cell Signalling Technology; 7074)
GAPDH	α-GAPDH mAb (Invitrogen; AM4300)	Mouse	α-mouse HRP-linked IgG, (Cell Signalling Technology; 7076)
GLUT4	α-GLUT4 pAb (Synaptic Systems; 235 003)	Rabbit	α-rabbit HRP-linked IgG, (Cell Signalling Technology; 7074)
IR	α-IRβ mAb (Abcam; ab69508)	Mouse	α-mouse HRP-linked IgG, (Cell Signalling Technology; 7076)
IGF-1R	α-IGF-1Rβ mAb (Cell Signalling Technology; 3018)	Rabbit	α-rabbit HRP-linked IgG, (Cell Signalling Technology; 7074)
PPAR-γ	α-PPARγ mAb (Santa Cruz; sc-7273)	Mouse	α-mouse HRP-linked IgG, (Cell Signalling Technology; 7076)

2.2.4 Bacterial transformation and storage

Bacterial transformation for the storage of recombinant 5' and 3' GLUT4 homology arm pSpCas9n(BB)-2A-Puro plasmids was performed with the use of NEB® 10-beta Competent *E. coli* (High Efficiency) (New England Biolabs; C3019H), following the full-length protocol (New England Biolabs, 2018). Cultures underwent antibiotic selection on LB agar plates with 100μg/ml ampicillin before liquid cultures were inoculated with individual colonies. Each culture was kept at -80°C in 8% DMSO for long-term storage.

2.3 Computational methods

2.3.1 Glucose nanosensor data acquisition

Fluorescent images from Förster resonance energy transfer (FRET) analysis of glucose uptake were provided by D. Kioumourtzoglou for Y201-derived adipocytes (n = 246) in the absence and presence of insulin at a range of stimulation time points. To generate numerical data from these images, the FRETzel programme was used (Wollman *et al.*, 2022). This programme allowed selection of cells from the series of images and returned the FRET ratio (the proportion of donor fluorophores that have excited an acceptor fluorophore) for each cell, serving as a metric to show the level of glucose uptake for each cell at each time point during insulin stimulation. Additional numerical data was provided by D. Kioumourtzoglou from 3T3-L1-derived adipocytes that had already been processed with FRETzel (n = 102)

2.3.2 FRET data analysis

The FRET ratios for each cell at time points from 0 to 20 minutes at 5 minute intervals were used to calculate a percentage change relative to the ratio value at 0 minutes for each individual cell. These percentage change values were compiled into a dataframe with each value categorised by time point of stimulation and type of cell. Analysis of these values was performed using the R software environment to generate graphical representations of the data. Statistical analysis of data points was performed using one-way ANOVA to identify differences in the average FRET ratio between either basal and insulin-stimulated cells of the same type at each time point, or between insulin-stimulated 3T3-L1-derived adipocytes and insulin-stimulated Y201-derived adipocytes at each time point. Data manipulation was facilitated with Tidyverse (Wickham *et al.*, 2019), and the readxl package (Wickham and Bryan, 2022).

2.3.3 PLA signal quantification

For the quantification of PLA signal, fluorescent microscope data was processed to generate maximum intensity projections. These images were imported into CellProfiler (Stirling *et al.*, 2021) and a pipeline was used to identify nuclei, plasma membranes, and fluorescent puncta indicative of a positive PLA signal. The total number of puncta per cell was calculated and exported as numerical data. This data was processed using R to perform statistical analysis in the form of one-way ANOVA to identify changes in PLA signal count between cell populations and time points of insulin stimulation. Data manipulation and graphical representation was performed using Tidyverse (Wickham *et al.*, 2019) and the readxl package (Wickham and Bryan, 2022).

Chapter 3: Results

3.1 Characterisation of adipogenesis in Y201 MSCs

3.1.1 Introduction

The capacity for MSCs to differentiate into adipocytes *in vivo* is well established (Robert *et al.*, 2020) but the molecular mechanisms involved in this process are not entirely understood. The present investigation aims to further our knowledge in this regard to develop a clearer picture of the pathways that drive adipogenesis, with a particular focus on IR and IGF-1R signalling. Suitable tools must be generated to facilitate this undertaking and will be employed at various stages throughout this investigation to provide a range of data to both characterise the ability of an alternative cell line (Y201 MSCs) to undergo adipogenesis, and to identify the roles of insulin receptor signalling in this process. The first part of this project will be focusing on Y201 MSC differentiation using a defined adipogenesis protocol (James *et al.*, 2015) to characterise this process and validate the use of Y201 MSCs in lieu of 3T3-L1 cells. These Y201 MSCs are regarded as an alternative cell line as a considerable proportion of studies investigating adipogenesis and related signalling mechanisms base their findings on the analysis of murine 3T3-L1 fibroblasts. Again the use of rodent models, either in terms of whole-organism or cell-based analyses, may not produce valid results in terms of human physiology or disease states due to significant differences in genetics, metabolism, and insulin signalling (Brillon *et al.*, 1988) between rodent and human models. Hence, the use of Y201 MSCs, a human cell line, is likely to provide more reliable and valuable information.

3.1.2 Analysis of Y201 MSC adipogenic potential

To better understand the physiological changes associated with the differentiation of Y201 MSCs into adipocytes, the proteomic and functional differences observed throughout this process must be analysed. This provides a baseline against which to compare any alteration in the differentiation potential of $IR^{-/-}$ and $IGF\text{-}1R^{-/-}$ MSCs. Hence, the expression of several adipocyte markers was analysed at weekly intervals during adipogenesis (Fig. 5A). The markers used for this include GLUT4, fatty acid-binding protein 4 (FABP4), and PPAR-γ. The facilitative glucose transporter GLUT4 is known to be highly expressed in adipocytes where it regulates glucose homeostasis in response to insulin, hence the decision to analyse its expression pattern. FABP4 and PPAR-γ are both well known adipocyte markers (Chu *et al.*, 2014; Matulewicz *et al.*, 2017; Robert *et al.*, 2020) and reflect the early and late stages of adipogenesis respectively. PPAR-γ is a key adipogenic transcription factor promoting the expression of genes for the regulation of processes such as lipid storage at the early stages of adipocyte differentiation (Ma *et al.*, 2018); FABP4 is

among these genes and plays a role in lipid metabolism in mature adipocytes (Furuhashi *et al.*, 2014). These results show a clear increase in expression of GLUT4 and FABP4 during adipogenesis as expected for mature adipocyte markers, and an increase and steady decrease of PPAR-γ expression characteristic of an early adipocyte marker. These results demonstrate successful adipogenesis based on changes in expression of each of the markers probed in this analysis. To further consolidate these findings and better characterise the changes observed throughout adipogenesis, the functional effects associated with this process must be investigated.

Lipid droplet accumulation is often used to assess the success of adipogenesis (Kraus *et al.*, 2016); oil red O staining is one way in which this analysis can be performed. Lipid droplets are membrane-bound organelles that form during adipogenesis (Franke, Hergt and Grund, 1987) in order to regulate the intracellular storage, metabolism, and mobilisation of lipids (Olzmann and Carvalho, 2019), and these organelles are abundant in mature adipocytes. Oil red O is a lipid-soluble stain, meaning that after its addition to fixed adipocytes and thorough washing of the cells, the dye is retained in the adipocytes' characteristic lipid droplets that accumulate during differentiation. These stained lipid droplets can then be visualised using visible light microscopy, providing a useful measure for the success of adipogenesis. Performing staining with this method allowed lipid droplets to be visualised throughout adipogenesis in this investigation (Fig. 5B). The observed increase in staining as time progressed confirmed the differentiation of MSCs into adipocytes. Taken together, these data provide evidence for the successful induction of adipogenesis in Y201 MSCs, and provide a foundation for the comparison of the differentiation capabilities of both $IR^{-/-}$ and $IGF\text{-}1R^{-/-}$ cell lines.

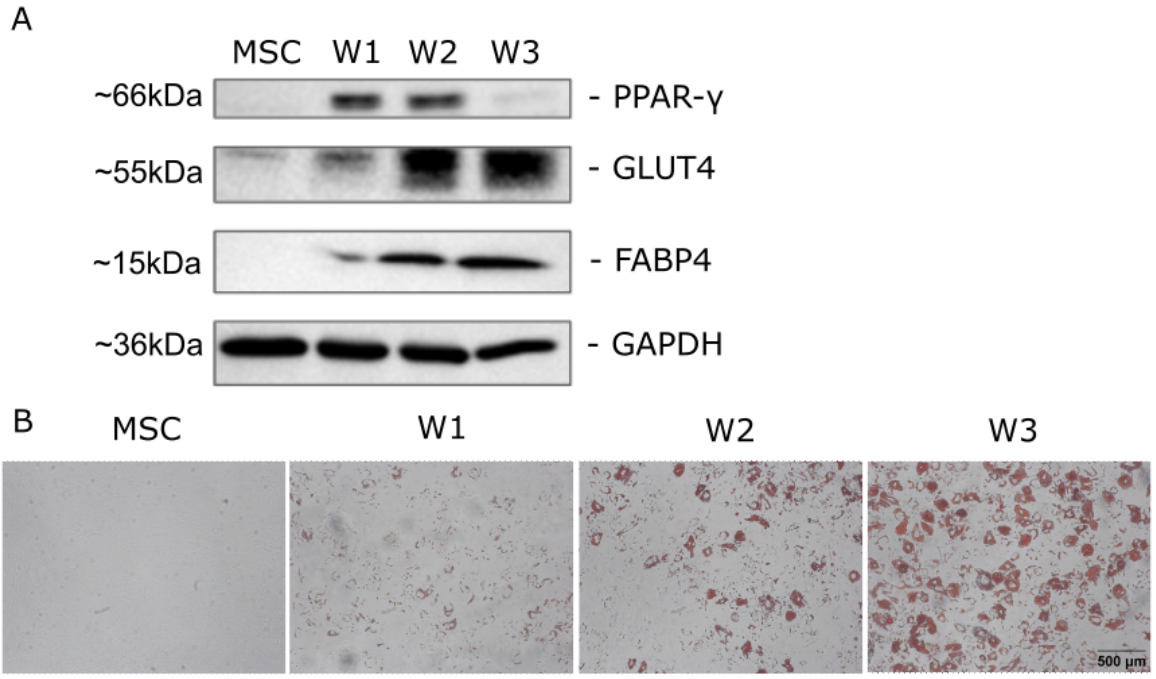

Figure 5: Proteomic and functional analysis of Y201 MSCs throughout adipogenesis. (A) Changes in expression of GLUT4, and early and late adipocyte markers PPAR-γ and FABP4 respectively at weekly intervals during adipogenic differentiation. **(B)** Oil red O staining of adipocytes at weekly intervals during adipogenic differentiation. Lipid droplets appear in red. 'W' denotes the week of differentiation, 'MSC' refers to undifferentiated Y201 MSCs.

3.1.3 Functional characterisation of Y201-derived adipocytes

While the proteomic and visual changes displayed by Y201 MSCs in the presence of adipogenic stimuli suggest successful differentiation, whether the adipocyte-like cells that form as a result of this stimulation exhibit the functional characteristics of primary adipocytes to a similar degree to that of 3T3-L1 adipocytes would confirm their validity and suitability as a model of insulin signalling in human adipocytes. The uptake of glucose via GLUT4 trafficking and facilitated diffusion in response to insulin receptor stimulation is a key process central to the function of adipocytes, and with relevance to this investigation with regard to insulin receptor signalling, this process was selected for the analysis of Y201-derived adipocyte function. Several techniques exist to monitor the cellular uptake of glucose, including the use of radiolabeled glucose, and fluorescent glucose analogues (Tanti *et al.*, 2001; Zou, Wang and Shen, 2005); the use of Förster resonance energy transfer (FRET) was employed in the present investigation for this purpose.

For the application of measuring glucose uptake, FRET was performed with the use of a chimeric protein comprising a glucose-binding region and two fluorophores, CFP (donor) and YFP (acceptor) (Fig. 6). These fluorophores have distinct excitation (Ex) and emission (Em) spectra but a considerable degree of overlap exists between the Em value of CFP and

the Ex value of YFP. It is this feature that underpins FRET; in the presence of glucose, the central protein binds glucose which induces a conformational change in the chimeric protein. This brings the two fluorophores in close proximity to one another to the extent that upon exposure to light at a wavelength equivalent to Ex_{CFP}, emitted energy in the form of CFP fluorescence is transferred to YFP. Due to the overlapping spectra, YFP becomes excited and fluoresces in turn. As this only occurs following a glucose-induced conformational change, the fluorescence of YFP can therefore be used as a metric to determine the cytosolic glucose levels, providing a way to assess the rate of glucose uptake in the cell and by extension, the rate of GLUT4 translocation and degree of metabolic insulin stimulation.

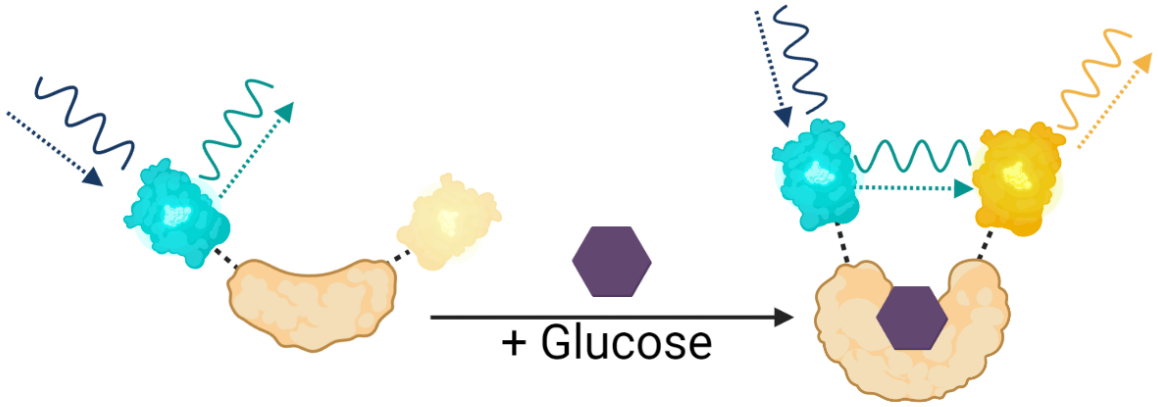

Figure 6: The chimeric glucose nanosensor used to quantify glucose uptake via FRET. Arrows accompanied by waves depict light of various wavelengths. The cyan and yellow fluorophores show CFP and YFP respectively.

Previously collected FRET data from both Y201-derived and 3T3-L1-derived adipocytes in the presence and absence of insulin was analysed at this stage in the investigation. Comparing these data allowed the relative glucose uptake in response to insulin stimulation to be identified in each cell line; it is apparent that both Y201 and 3T3-L1 adipocytes respond in a similar fashion upon exposure to insulin, showing increasing FRET signals with increasing insulin stimulation duration, indicative of increased glucose uptake (Fig. 7A). Moreover, comparing each cell type in the presence of insulin shows a very similar pattern of FRET signal change; when comparing the absolute change in FRET signal, no significant difference is found between the insulin response of the two cell types (Fig. 7B) which lends credence to the suitability of Y201-derived adipocytes as a suitable alternative to 3T3-L1-derived adipocytes in the context of the metabolic insulin response. However, taking the basal control into consideration for each cell type exposes a significant difference in the FRET signal at the 5 and 10 minute time points before the data levels out and each cell type demonstrates a similar rate of glucose uptake. These data show a comparable metabolic insulin response of adipocytes derived from each cell line but highlights a difference in the rate of glucose uptake at earlier time points of insulin stimulation.

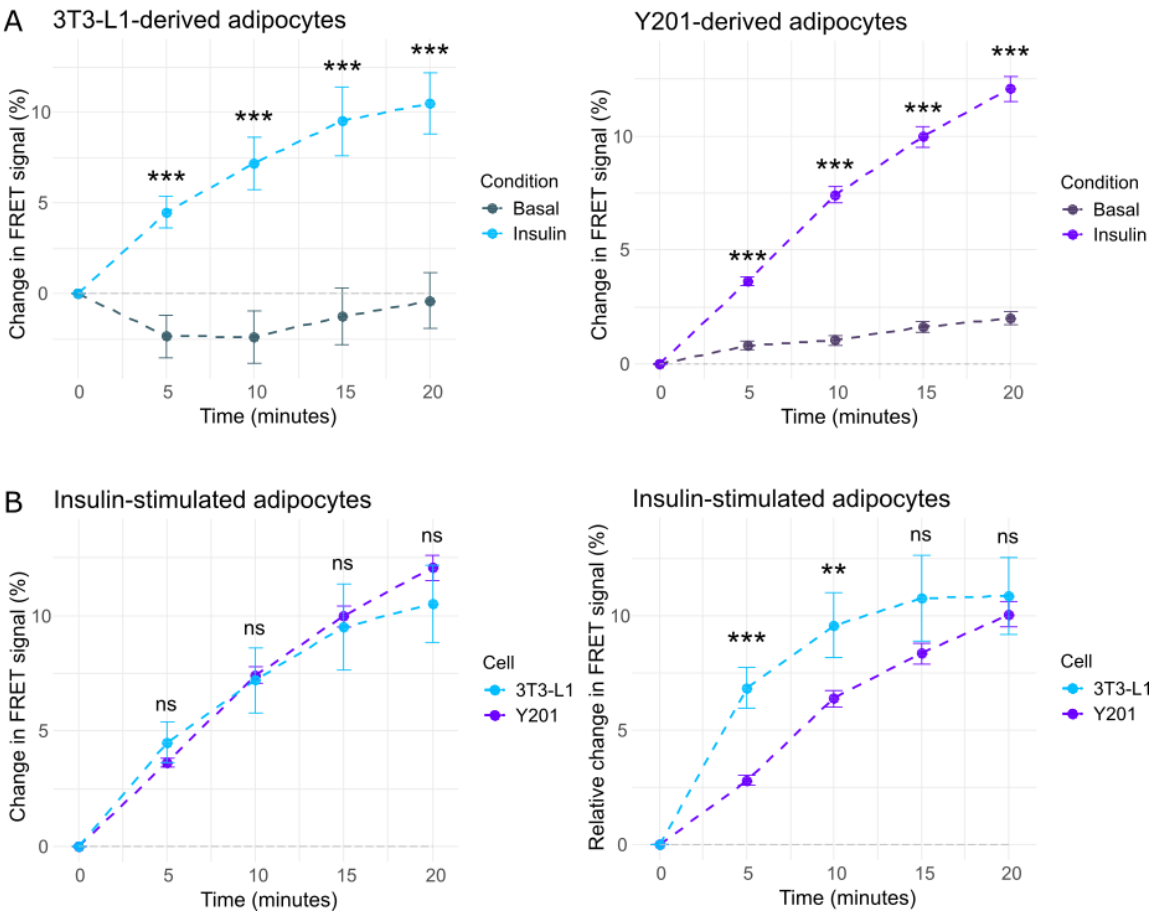

Figure 7: Comparison of FRET signal data from 3T3-L1 fibroblast-derived adipocytes and Y201 MSC-derived adipocytes. (A) Percentage change in FRET signals of insulin-stimulated or unstimulated (basal) 3T3-L1-derived adipocytes (left) and Y201-derived adipocytes (right). Basal conditions serve as a baseline for the rate of glucose uptake. **(B)** Percentage change in FRET signals of each group of insulin-stimulated adipocytes shown as absolute values (left) or relative to the basal levels from (A) (right). Time points specify the duration of insulin stimulation for each group of stimulated cells or measurements from the same time point in unstimulated cells. Error bars denote SEM. '***' denotes significance at $P < 0.001$, '**' denotes significance at $P < 0.01$, 'ns' denotes no significance.

3.2 Analysis of IR/IGF-1R profile throughout adipogenesis

3.2.1 Identification of changes in expression of IR and IGF-1R

Insulin is known to play an important role in adipogenesis as key driver of this process (Klemm *et al.*, 2001; Cignarelli *et al.*, 2019), further demonstrated by its use as an adipogenic induction agent in the present investigation (Pittenger *et al.*, 1999). With downstream targets such as SREBP-1c and mTORC1 associated with the activation of lipogenesis and the inhibition of lipolysis respectively (Foretz *et al.*, 1999; Dif *et al.*, 2006; Chakrabarti *et al.*, 2013), the receptors activated by insulin signalling are essential for mediating insulin's upregulatory effects on adipogenesis as a whole. With no clear idea of

the insulin receptors involved in promoting adipogenesis, it is critical to identify how the expression of each receptor's cognate gene changes throughout this process to better understand the importance of these receptors in the differentiation of MSCs into adipocytes. To explore this, the receptor content of Y201 MSCs and Y201-derived adipocytes at week 3 of differentiation was compared (Fig. 8) It is clear from this proteomic analysis that the expression of *INSR* remains constant before and after adipogenesis. Expression of *IGF-1R*, however, appears to be significantly curtailed in adipocytes due to a notable decrease in the levels of IGF-1R protein following differentiation. This information indicates the relative importance of each of these receptors in the function of MSCs and adipocytes and may hint to their roles in adipogenesis.

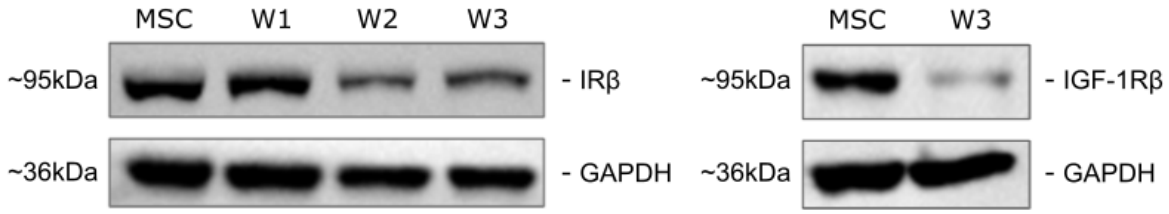

Figure 8: IR and IGF-1R expression changes during adipogenesis. IR protein content in Y201 MSCs before, and at weekly intervals during, induced adipogenesis (left), and IGF-1R protein content in Y201 MSCs before and after induced adipogenesis (right). 'W' denotes the week of differentiation, 'MSC' refers to undifferentiated Y201 MSCs.

3.2.2 Identification of heterodimeric receptor formation

With insulin receptor monomers displaying promiscuity in their interactions and forming a range of heterodimeric receptors, it remains to be evaluated whether these receptor hybrids have any influence on the ability of cells to differentiate into adipocytes. A proximity ligation assay (PLA) was used to elucidate the potential involvement of IR/IGF-1R hybrids in adipogenesis by determining the change in their abundance throughout the process. PLA utilises specific monoclonal antibodies to detect the spatial juxtaposition of two epitopes, such as is found on two separate but interacting proteins (Fig. 9). These primary antibodies, raised in different species, bind to their target epitopes before the addition of secondary antibodies known as PLA probes. PLA probes are secondary antibodies conjugated to oligonucleotides that, once bound to primary antibodies in close proximity, interact with connector oligonucleotides that result in the formation of a circular DNA amplification template. At this stage, one of the PLA probes acts as a primer for DNA polymerase leading to amplification of DNA at the site of protein interaction. The newly-synthesised amplicon is then labelled for detection and observed using confocal microscopy whereby individual heterodimeric receptors can be visualised as distinct puncta.

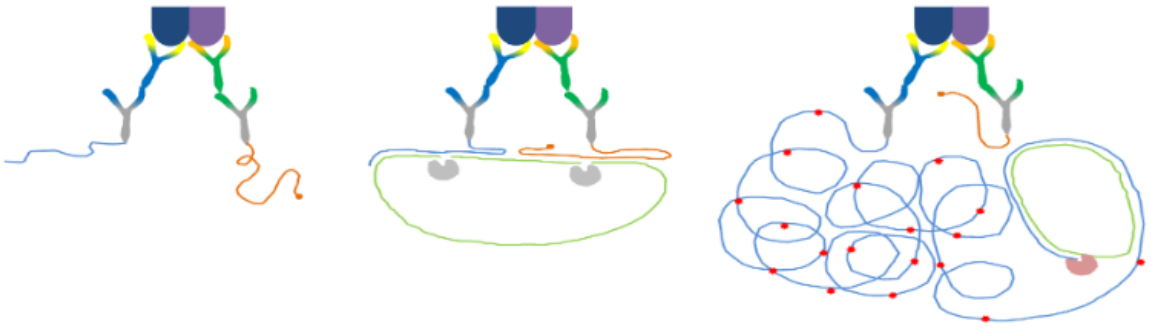

Figure 9: The PLA system used for detection of IR/IGF-1R heterodimers. Primary antibodies bind epitopes on the intracellular IR and IGF-1R domains (dark blue, purple) and become bound by secondary antibodies with conjugated oligonucleotides (blue, orange) (left). These oligonucleotides are complementary to connector oligonucleotides (light green) that form circular ssDNA after the action of DNA ligase (grey) (middle). The circular DNA template allows amplification of one of the antibody-conjugated oligonucleotides (blue) by DNA polymerase (pink) and incorporation of fluorophores (red) (right).

PLA was used at this stage of the investigation to identify adipogenesis-associated changes in the formation of heterodimers comprising IGF-1R bound to either of the IR monomers. To transmit intracellular signals, many RTKs similar to IRs and IGF-1R undergo ligand-mediated dimerisation (Schlessinger, 2000; Liu *et al.*, 2007; Leppänen *et al.*, 2010), as opposed to being present at the plasma membrane in an inherently dimeric form. To ensure the IR/IGF-1R dimers were present, some groups of cells to be analysed via PLA were stimulated with insulin prior to being fixed. At this stage, PLA enabled visualisation of the IR/IGF-1R hybrids (Fig. 10), and quantification of the abundance of these receptors before and after differentiation and at various time points of insulin stimulation.

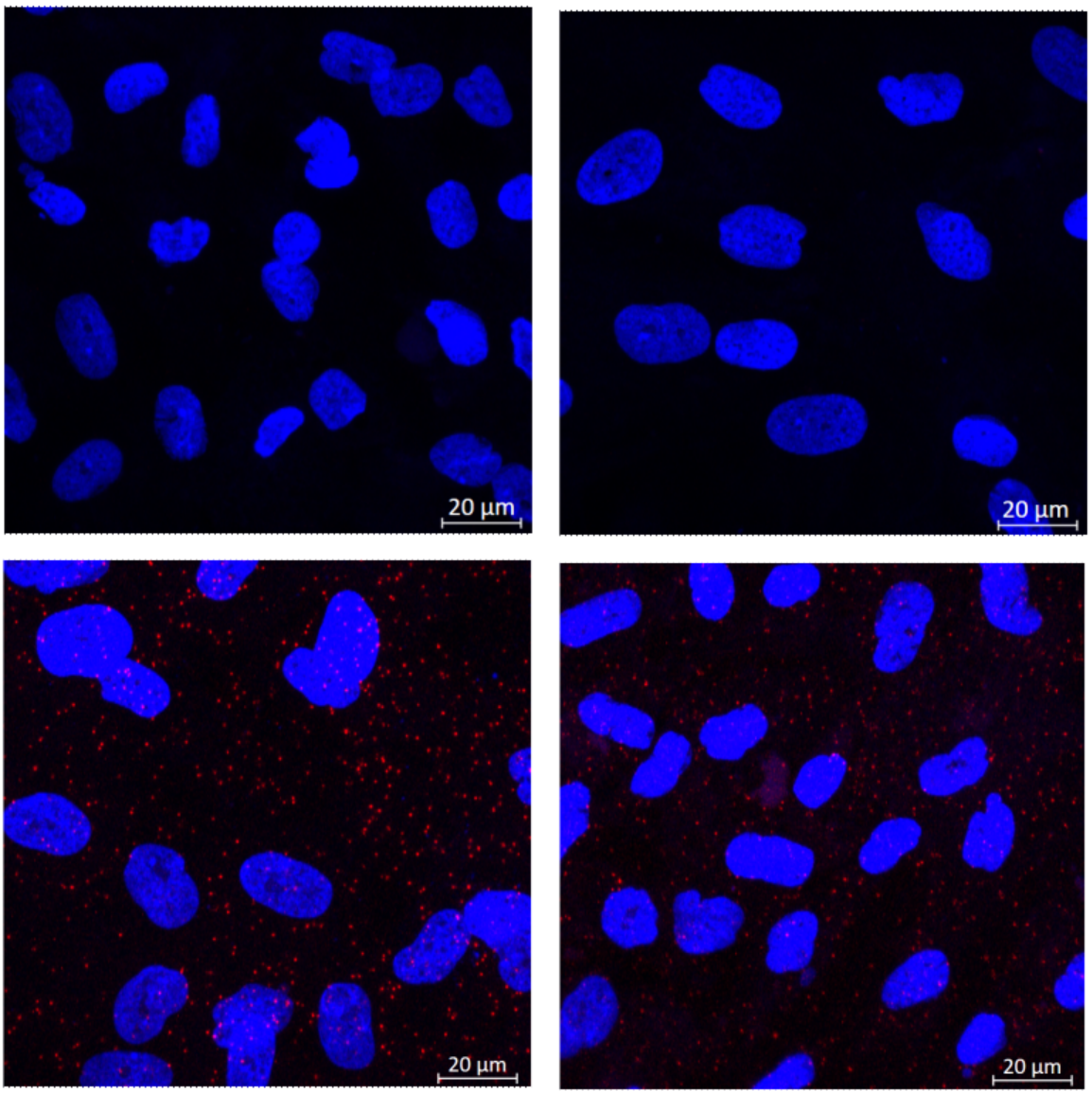

Figure 10: Visible PLA signal in Y201 MSCs and Y201-derived adipocytes. Signal seen via confocal microscopy in Y201-derived adipocytes with the use of IR-only (top left) and IGF-1R-only (top right) primary antibodies, and in the presence of both antibodies in Y201 MSCs (bottom left) and Y201-derived adipocytes (bottom right). All groups in these images were stimulated with insulin for 10 minutes prior to PFA fixation. Blue fluorescence = DAPI, red fluorescence = PLA signal.

In both MSCs and adipocytes, the abundance of IR:IGF-R heterodimers appears to decrease with great significance within 5 minutes of insulin stimulation (Fig. 11A). This is followed by a steady increase in PLA signal up to the 20 minute stimulation time point in MSCs to the extent that no significant difference is seen between this value in MSCs at 20 minutes and 0 minutes of insulin stimulation. However, PLA signal count steadily decreases across the same period in adipocytes. When comparing PLA signal between cell types at 0 minutes and 5 minutes of insulin stimulation, MSCs display a significantly higher number of IR:IGF-1R heterodimers (Fig. 11B). Of particular note is the difference in the decrease of PLA signal count between cell groups at each time point. Mean PLA signal at basal

conditions is 101 puncta in MSCs and 63 puncta in adipocytes; following 5 minutes of insulin stimulation, mean PLA signal count is 76 in MSCs and 15 in adipocytes. These data clearly suggest a difference in hybrid receptor formation and abundance following adipogenesis and after varying durations of insulin stimulation of either cell group.

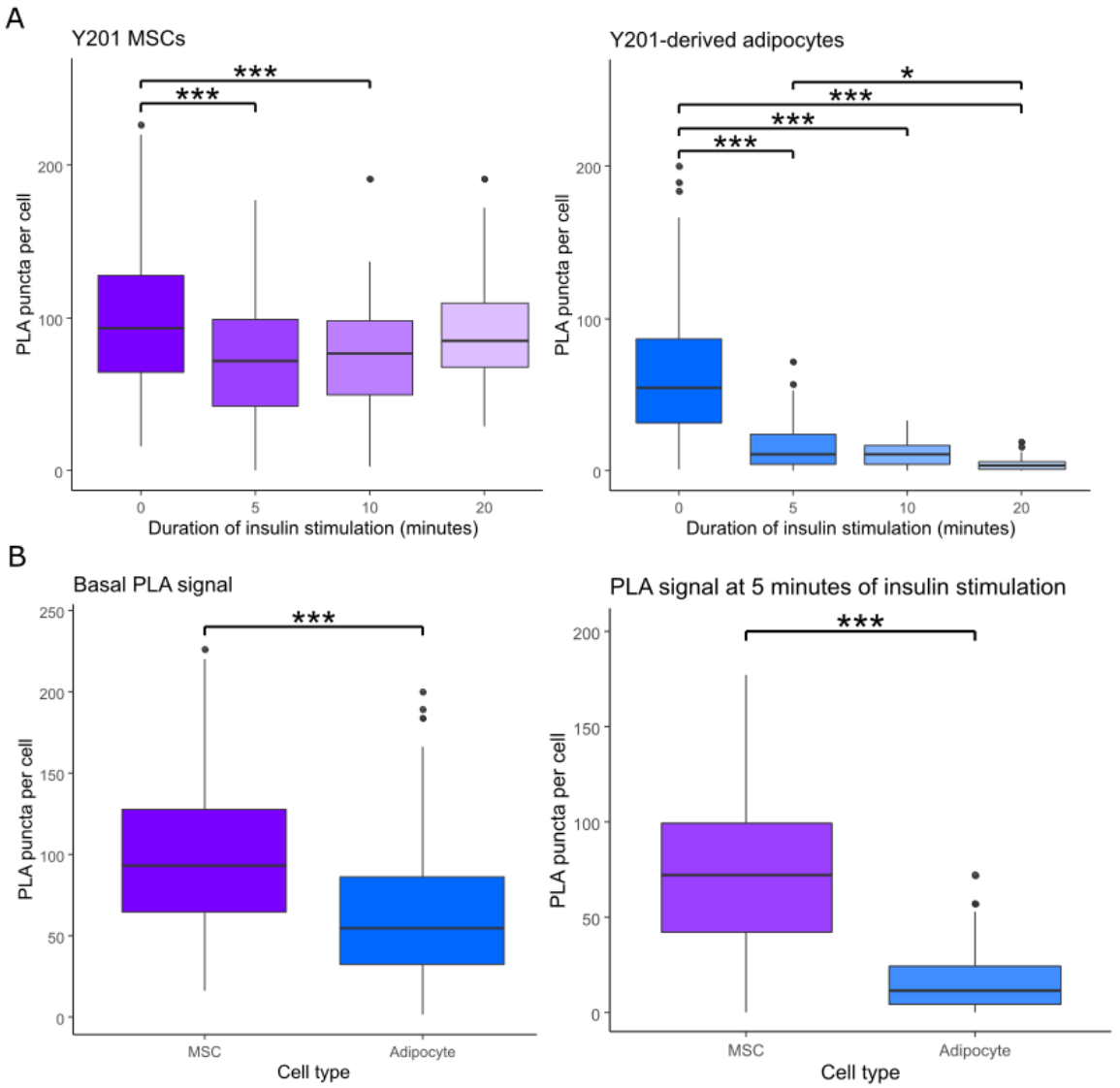

Figure 11: Quantitative analysis of PLA signal. (A) Number of puncta per cell following PLA at each time point of insulin stimulation in Y201 MSCs (left) and Y201-derived adipocytes (right) **(B)** Comparison of PLA signal between unstimulated Y201 derived MSCs and unstimulated Y201-derived adipocytes (left) and both groups following 5 minutes of insulin stimulation (right). '***' denotes significance at $P < 0.001$, '*' denotes significance at $P < 0.05$. Outliers are represented by grey points.

3.3 Generation of IR and IGF-1R knockouts

3.3.1 CRISPR-Cas9-directed deletion of *INSR* and *IGF-1R*

The proceedings of this investigation rely somewhat on the acquisition of Y201 MSCs expressing only one of either the *INSR* or *IGF-1R* genes. These cells would prove invaluable in the ability to determine the capacity of each insulin-binding receptor (IRs compared to IGF-1R) to support adipogenesis and identify the potential roles of these receptors in disease states such as obesity. For this purpose, a CRISPR-Cas9-based approach was taken to selectively knock out each of these genes to generate two novel cell lines with the aforementioned receptor profiles. CRISPR-Cas9 is an effective tool with regard to genome editing; this system possesses the ability to selectively knock out endogenous genes or to insert exogenous sequences into the host cell genome for ectopic gene expression (Ran *et al.*, 2013). Gene knockout in this manner is mediated by the Cas9 protein in the presence of single guide RNA (sgRNA) but in the absence of a repair template. This aims to induce the formation of a DNA double-stranded break (DSB) at the location specified by the sgRNA to be repaired by intrinsic cellular mechanisms via non-homologous end joining (NHEJ). This interrupts the sequence of nucleotides which suppresses transcription and effectively deletes the targeted gene. Although powerful, this tool is not 100% effective; factors such as questionable fidelity of the Cas9 protein to the sgRNA target (Hsu *et al.*, 2013) and complex Cas9-DNA interaction kinetics (Q. Zhang *et al.*, 2019) may lead to off-target enzymatic activity and unsuccessful gene knockout. Hence, when using this tool to engineer cells, it is sensible to edit a large number of cells to ensure at least one successful edit has been performed by Cas9.

The attempted generation of $IR^{-/-}$ and $IGF\text{-}1R^{-/-}$ Y201 MSCs in this investigation was facilitated by the use of CRISPR-Cas9. For this purpose, plasmids encoding Cas9, sgRNA targeting *INSR* or *IGF-1R*, and RFP were used in the transfection of Y201 MSCs. Consequently, cells successfully transfected with one of these plasmids expressed RFP at variable levels (Fig. 12). Fluorescent cells were isolated and expanded to generate clonal colonies of knockout candidates for each gene. All candidates underwent proteomic screening at this stage to identify potential success of CRISPR-Cas9 editing; this mass screening aimed to account for the aforementioned factors influencing the results of Cas9-directed gene deletion by analysing a large number of knockout candidates. The screening process identified several promising knockout candidates (Fig. 13A) which, due to issues with sample loading and membrane transfer in this first screening, underwent additional screening to confirm gene deletion (Fig. 13B).

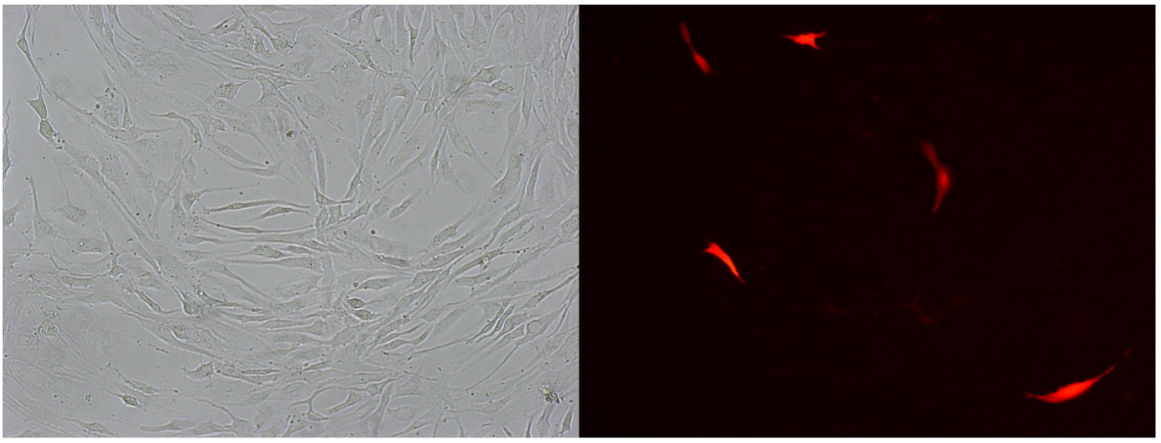

Figure 12: RFP fluorescence following successful transfection of an RFP-tagged Cas9 plasmid. Y201 MSCs transfected with an RFP-tagged *INSR*-targeted CRISPR-Cas9 construct for the generation of *INSR*$^{-/-}$ cells, viewed with bright field (left) and fluorescence (right) microscopy.

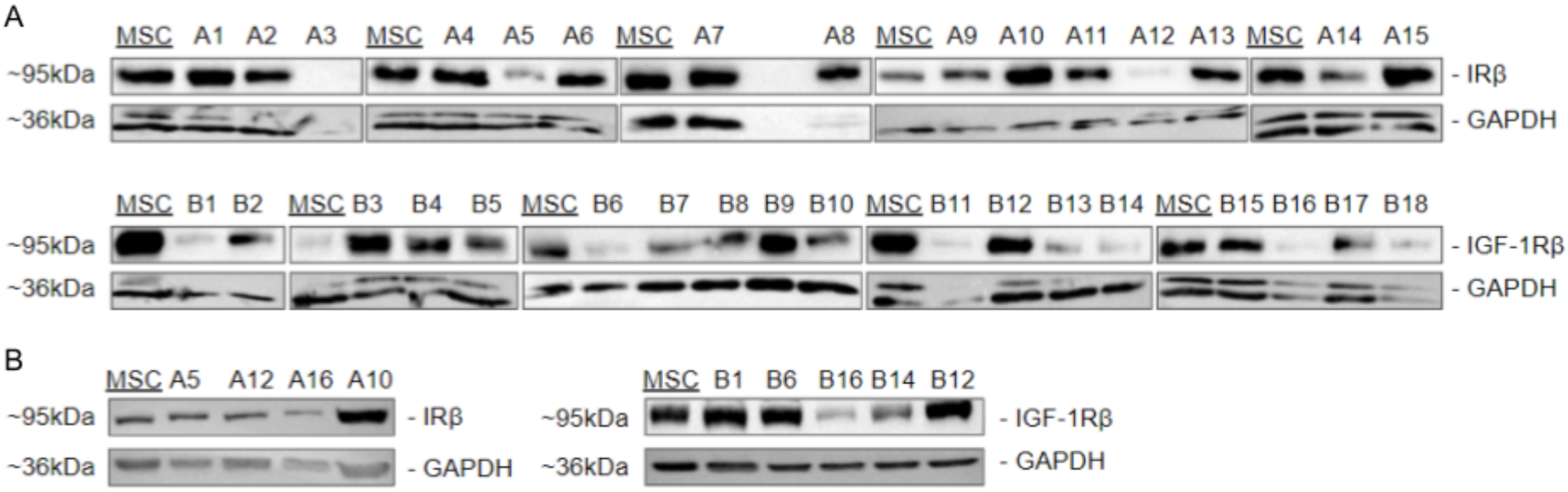

Figure 13: IR and IGF-1R protein content of *INSR* and *IGF-1R* knockout candidates. (A) Detection of β chains of IR (top) and IGF-1R (bottom), representative of expression levels of whole IR and IGF-1R proteins in each knockout candidate screened. **(B)** Second screening of knockout candidates for IR (left) and IGF-1R (right). *INSR*$^{-/-}$ candidate A16 refers to a candidate not originally screened in the present investigation. *INSR*$^{-/-}$ candidate A10 and *IGF-1R*$^{-/-}$ candidate B12 serve as additional controls in this second screening. MSC refers to unmodified Y201 MSCs used for demonstration of physiological IR and IGF-1R levels. A and B refer to individual numbered clonal colonies generated from single cell expansion of cells successfully transfected with Cas9 constructs targeting *INSR* and *IGF-1R* respectively.

3.3.2 Generation of a modified GLUT4 construct for future functional analysis

As a major effector of insulin receptor signalling, GLUT4 plays a significant role in both cellular and whole-body glucose homeostasis. This facilitative glucose transporter, sequestered in intracellular storage vesicles under basal conditions, undergoes translocation and is presented on the plasma membrane in the presence of an insulin stimulus, allowing an influx of glucose from the blood to the cytoplasm. This translocation of GLUT4 to the plasma membrane is clearly crucial for the function of this protein and the metabolic insulin signalling pathway as a whole and it is this mechanism that can serve as a useful reporter of insulin receptor signalling efficiency.

By generating a GLUT4 construct tagged with a fluorescent protein (GFP) and a glycoprotein (HA), the trafficking of GLUT4 storage compartments to the plasma membrane can be visualised. This protein was designed in such a way that, once present on the plasma membrane, the fluorescent GFP tag is positioned intracellularly whereas the HA is located outside of the plasma membrane (Fig. 14A). This arrangement means GLUT4 stored in intracellular compartments can be observed via GFP fluorescence, and plasma membrane-localised GLUT4 can be observed using fluorophore-conjugated α-HA antibodies. This would allow visualisation of GLUT4 translocation which could be used as a measure of insulin signalling responsiveness in the absence of either IR or IGF-1R to determine the capacity of each of these receptors to transduce metabolic insulin signals.

The goal of using this method is to replace the endogenous GLUT4 locus, *SLC2A4*, with the double-tagged construct. This would be facilitated via use of CRISPR-Cas9-directed genomic insertion of a linear piece of DNA encoding the HA-GLUT4-GFP construct. Similarly to the Cas9-directed knockout mechanism discussed in section 3.3.1, this technique involves the formation of breaks in the DNA in the presence of a repair template encoding the exogenous gene (HA-GLUT4-GFP in this case) to be inserted. This template is included with the aim of promoting homology-directed repair (HDR) rather than NHEJ. HDR is a DNA repair mechanism that only occurs in the presence of a homologous repair template but occurs at a lower frequency than NHEJ due to a number of factors influenced by the gene and cell type involved (Ran *et al.*, 2013). This means the success of using CRISPR-Cas9 for the insertion of exogenous sequences is generally lower than is seen when using the tool for NHEJ-mediated gene knockout.

Although this analysis was not performed in the present investigation, the plasmids required for genomic insertion of this GLUT4 construct were generated. Three separate plasmids are required for insertion of the HA-GLUT4-GFP construct, two of which were generated as part of this investigation. These two plasmids encode Cas9 proteins with

either the 5’ or 3’ homology arm to serve as sgRNA for the generation of DNA lesions in *SLC2A4*, as well as a puromycin resistance gene (*PuroR*) to serve as a selectable marker for downstream optimisation of transfection and subsequent gene insertion. The transfection potential for these plasmids was confirmed in this investigation with the generation of identical plasmids encoding GFP rather than PuroR and subsequent transfection of Y201 MSCs (Fig. 14B); the observed GFP fluorescence is indicative of successful transfection and demonstrates the feasibility of using the PuroR-encoding plasmids in future. This will prove valuable for future isolation of cells transfected with these plasmids to generate a cell line expressing the HA-GLUT4-GFP construct by enabling puromycin selection prior to clonal expansion and stabilisation of the new cell line. The HA-GLUT4-GFP plasmid was readily available at the beginning of this investigation and awaits cotransfection with the two aforementioned plasmids for its insertion into the Y201 MSC genome.

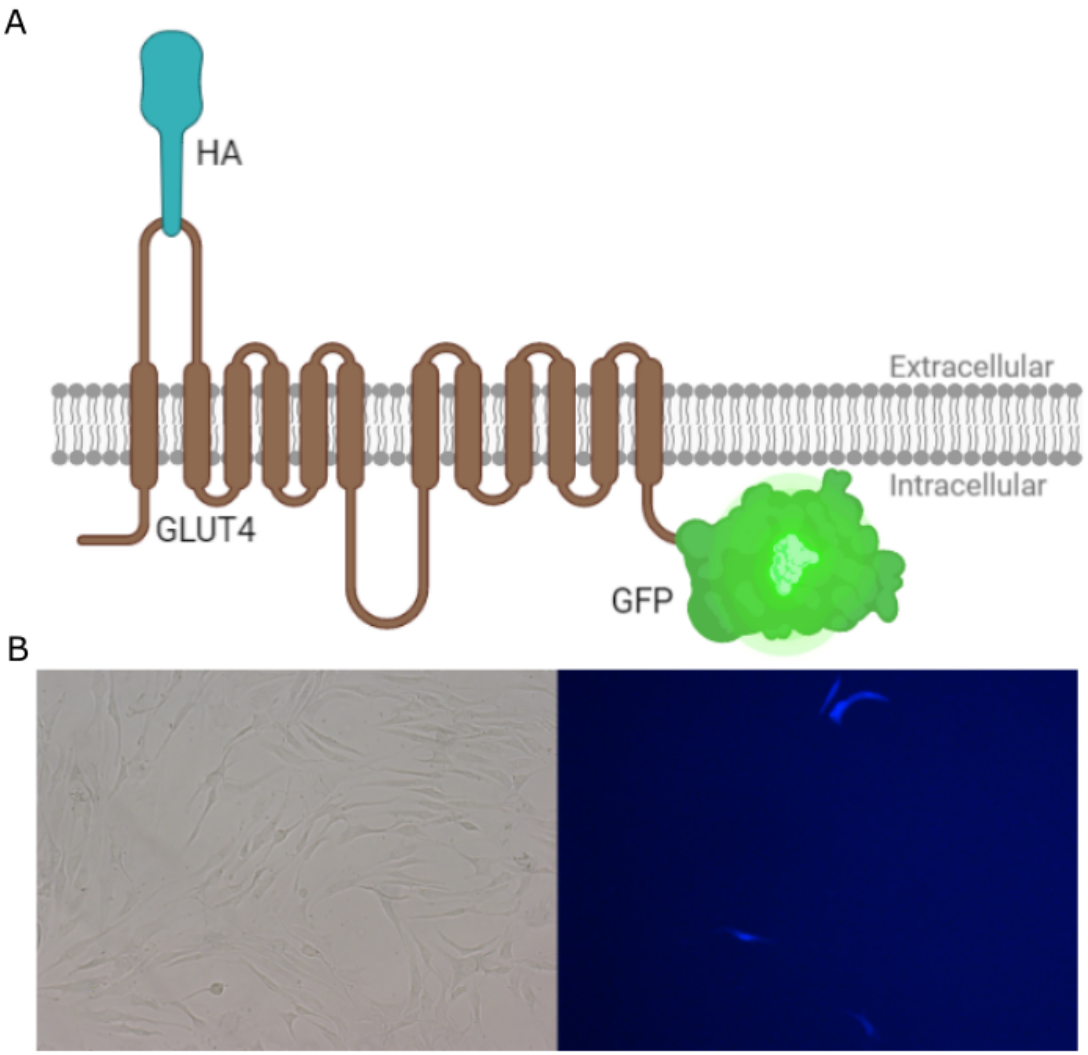

Figure 14: GFP fluorescence following successful transfection of a GFP-tagged, *SLC2A4*-targeted Cas9 plasmid. (A) The protein construct encoded by the GFP-tagged *SLC2A4*-targeted Cas9 plasmid. **(B)** Y201 MSCs transfected with a GFP-tagged CRISPR-Cas9 construct that will enable downstream analysis of metabolic responses to insulin signalling, by facilitating replacement of the *SLC2A4* locus with the double-tagged GLUT4 construct. Images viewed with bright field (left) and fluorescence (right) microscopy.

Chapter 4: Discussion

4.1 Investigation summary

T2DM is a widespread global disease with severe consequences for those affected. The exponentially increasing prevalence of T2DM and the links between this disorder and other disease states such as obesity and cancer make it an increasingly important condition to be focused on by modern biomedical research. The key factor responsible for the overlap between these three disease states is insulin signalling, the pathways associated with which play major roles in cellular metabolism, adipogenesis, and cell proliferation. To identify and better understand the drivers of each of these cellular responses, the intracellular pathways leading to these effects must be disentangled. With six major receptors expressed in a multitude of cells, it is expected that insulin would possess the ability to modulate such a diverse array of cellular signalling pathways; whether this multiplicity of receptors is a determinant of the cellular response generated by insulin is not fully understood. Hence, feeding into the overall aim of delineating the signalling pathways emanating from each insulin receptor, this project aimed to investigate the various receptors for insulin on an independent basis in an attempt to identify whether any preferential pathway activation could be observed with respect to each receptor. Such an ambitious undertaking as uncoupling all pathways involved in the disease states linked to insulin signalling in the context of all six receptors would necessitate a greater time frame for experimental research so, to pursue an achievable but no less consequential goal within the scope of this project, the role of several insulin receptors was to be characterised in the context of adipogenesis. In addition, this project aimed to characterise an alternative cell line in the context of adipogenesis to determine its suitability for future investigations focusing on the human insulin signalling pathway.

Several noteworthy results were obtained from the present investigation, which help to answer the questions posed by this project's aims i.e. how are the various receptors for insulin involved in the differentiation of MSCs into adipocytes, and how appropriate are Y201 MSCs for the characterisation of human adipogenesis; could they serve as a suitable platform for future investigation of T2DM and cancer? Apropos of future work, the undertakings of this project also generated a tool for analysis of the metabolic pathways associated with insulin receptor signalling, which will prove invaluable in unravelling the entwined signalling pathways downstream of insulin receptor stimulation. To summarise the key findings of this work, it was shown that induction of adipogenesis in Y201 MSCs resulted in the characteristic proteomic and functional changes seen following differentiation of the 3T3-L1 fibroblasts widely-used for modern studies of adipogenesis and insulin signalling. The changes in receptor expression and heterodimeric receptor formation were also analysed to build a better picture of the potential roles of each

receptor investigated in adipogenesis and adipocyte function. Finally, several promising *INSR*$^{-/-}$ and *IGF-1R*$^{-/-}$ candidates were identified following transfection of the RFP-tagged CRISPR-Cas9 constructs but second screening of these candidates suggests unsuccessful knockout; this will need further validation with additional screening techniques.

4.2 Interpretation of key results

4.2.1 Y201 MSCs are suitable for the investigation of adipogenesis

Y201 MSCs were used as an alternative cell line to 3T3-L1 fibroblasts in this investigation due to their physiological relevance to human disease states. As discussed, 3T3-L1 fibroblasts are murine cells and, for several reasons, may therefore not be accurate in the investigation of human T2DM or obesity, despite their common use throughout biomedical investigations in these contexts. The validation of this cell line, firstly by analysis of its capacity to undergo induced adipogenesis by identifying changes in adipocyte marker expression (Fig. 5A), yielded results expected in successful adipogenesis. As stated in section 3.1.2, the steadily increasing expression of late adipocyte markers FABP4 and GLUT4, and sudden increase and slow decrease of early adipocyte marker PPAR-γ over 21 days demonstrates successful adipogenesis. This suggests the proteomic changes undergone by Y201 MSCs upon stimulation with adipogenic induction media to be proteomically similar to those seen in 3T3-L1 fibroblasts, already making them a promising alternative to these murine cells. Further consolidating these findings, ORO staining of Y201 MSCs throughout adipogenesis (Fig. 5B) demonstrated clear accumulation of lipid droplets as expected for cells differentiating into adipocytes. It is known that energy surplus, such as would be seen with increased glucose flux, promotes energy storage in the form of lipid droplet accumulation (Stenkula and Erlanson-Albertsson, 2018); the increase in GLUT4 expression (Fig. 5A) throughout adipogenesis may therefore explain the increase in visible lipids throughout differentiation (Fig. 5B).

As well as the proteomic changes, it remained to be seen whether the functionality of Y201 MSCs was comparable to that of 3T3-L1 adipocytes. In this case, functionality was determined by the ability of each of these cell lines to uptake glucose in response to insulin. This glucose uptake, measured using the FRET-based glucose nanosensor (Fig. 6), acted as a reporter for GLUT4 translocation following insulin stimulation of each of these cell lines. It was immediately evident upon analysis of the nanosensor data that both Y201-derived adipocytes and 3T3-L1-derived adipocytes respond to insulin in a similar fashion with respect to glucose uptake, displaying a significant increase relative to basal levels for all time points measured (Fig. 7A). The basal values for glucose uptake measured in unstimulated cells follow very different trajectories for each cell type. The

reason for this is unknown but could be a result of issues such as high sensitivity of the FRET system which would imply that only values over a certain threshold should be considered as different from this baseline. Moreover, with the FRET detection method depending upon emission of light through a liquid, slightly differing liquid volumes used in this analysis could refract light unpredictably and lead to loss of signal which would explain the discrepancy between the baselines for each cell group. It should also be noted that the error bars for 3T3-L1-derived adipocytes appear much greater than those of Y201-derived adipocytes, indicating a wider spread of data and greater uncertainty of the true mean. These factors may explain the variability in basal values.

Interestingly, despite the almost identical correlation of absolute glucose uptake levels in both stimulated cell groups (Fig. 7B), when accounting for the variable basal levels of glucose uptake, Y201-derived adipocytes exhibit a significantly lower level of glucose uptake at 5 and 10 minutes of insulin stimulation compared to 3T3-L1-derived adipocytes. Following this discrepancy, Y201-derived adipocytes appear to reach comparable levels of glucose uptake at the later time points used for this analysis. This finding was unexpected and the cause of this pattern has not been established; it suggests a difference in the rate of GLUT4 translocation at earlier time points of insulin stimulation compared to that observed at later time points. One reason this could arise is due to the regulation of the early and late metabolic insulin response. Separating the response in this way into two separate phases would point to differential regulation of the GLUT4 trafficking pathway in Y201-derived adipocytes relative to 3T3-L1-derived adipocytes.

With these differences in mind, and considering that 3T3-L1 fibroblasts are commonly used for analysis of glucose metabolism and adipogenesis, it may appear that Y201 MSCs are less suitable than 3T3-L1 fibroblasts for analysis of the insulin signalling pathways involved in these processes. On the contrary, it is crucial to remember that Y201 MSCs are a human cell line and any differences between human and murine cells highlight the existence of differences in the many cellular mechanisms between humans and rodents (Brillon *et al.*, 1988). Hence, although different from 3T3-L1 fibroblast results, these results obtained from the use of Y201 MSCs are likely to provide a more accurate model of human insulin signalling pathways and any links made to human disease states may automatically be more valid than when using murine cells.

4.2.2 Receptor expression patterns exemplify differential function

Although insulin is known to play a key role in promoting adipogenesis, the expression of IR and IGF-1R in Y201 MSCs throughout adipogenesis has not been characterised. It is crucial to identify any changes in this process to gain a first insight into the potential involvements of each receptor in the differentiation of adipocytes; it has been demonstrated that Y201 MSCs can undergo adipogenesis successfully based on the

changes in adipocyte marker expression (Fig. 5A) and this stage of the investigation aims to explore this with respect to insulin-binding receptors. In summary, IR content appears to remain mostly stable relative to the GAPDH loading control with a potential slight decrease in expression between weeks 1 and 2 of induced adipogenesis (Fig. 8). With the metabolic regulation of adipocytes considered one of the major functions of insulin receptor signalling (Tokarz, MacDonald and Klip, 2018), it was expected that the absolute levels of IR expression would either increase or remain entirely unchanged when comparing Y201 MSCs with Y201-derived adipocytes. Interestingly, it has been reported that IR signalling is a key regulator of stem cell pluripotency and lineage determination (Gupta *et al.*, 2018). With Y201 MSCs classed as multipotent stem cells, this may explain the slightly higher expression of IR in Y201 MSCs than Y201-derived adipocytes.

The content of IGF-1R was, due to technical issues in the acquisition of this result, only analysed before and after adipogenesis and not at weekly intervals throughout the process. It is clear that IGF-1R expression decreases dramatically during differentiation as the levels of this protein are much greater in Y201 MSCs than in Y201-derived adipocytes (Fig. 8). It is important to remember that insulin is not the primary ligand for IGF-1R and that this receptor has its own function irrespective of insulin signalling. This is likely the reason for its expected higher expression in Y201 MSCs where the protein is involved in the transduction of IGF-1 signals to promote the growth and proliferation of these stem cells (Teng, Jeng and Shyu, 2018). With the regulation of stem cell proliferation its main role, it is unusual that this protein is still expressed at a low but no less noticeable level in adipocytes, these terminally-differentiated and, in contrast to MSCs, relatively dormant cells would not be expected to undergo proliferation and therefore IGF-1R expression would presumably reduce to nothing. However, this understanding of adipocyte function is a misunderstanding and several studies have shown that these mature cells can, in fact, proliferate, albeit at a much lower rate than stem cells, and are known to secrete growth factors such as IGF-1 which may act via autocrine or paracrine signalling (Sugihara *et al.*, 1987; Hausman *et al.*, 2001). This alone could explain the low level of IGF-1R expression in Y201-derived adipocytes but this receptor could promote additional cellular functions in response to insulin.

4.2.3 Heterodimeric receptor abundance varies during adipogenesis and insulin stimulation

To expand upon the function of IR and IGF-1R in MSCs and adipocytes, it remained to be seen how the observed heterodimerisation of these receptors' monomeric constituents changed throughout adipogenesis. Only with the use of PLA has the propensity for the receptor subunits to heterodimerise been ascertained. The images obtained from confocal microscopic analysis of the cells that underwent PLA serve as a control to demonstrate

successful execution of the PLA (Fig. 10). No puncta with fluorescence greater than that of the background were detectable in the two samples that used each primary antibody in isolation. Combined with the clear puncta in the two samples exposed to both primary antibodies, these images show that IR:IGF-1R heterodimeric receptors are present and detectable in both Y201 MSCs and Y201-derived adipocytes fixed after 10 minutes of insulin stimulation.

Quantification of PLA signal from similar such images obtained from the remaining samples revealed several interesting features of IR:IGF-1R heterodimer abundance. The first notable difference is the lower PLA signal in adipocytes compared to MSCs, representative of a lower number of IR:IGF-1R heterodimers per cell. This could be explained by the lower expression of IGF-1R in Y201-derived adipocytes (Fig. 8). One particularly unexpected finding concerned the influence of insulin on heterodimer formation. Considering that IR and IGF-1R are both RTKs and that many RTKs dimerise only upon encountering their cognate ligand (Schlessinger, 2000; Liu *et al.*, 2007; Leppänen *et al.*, 2010), it was anticipated that with increasing durations of insulin stimulation, the average number of PLA puncta would increase. This would indicate increasing IR:IGF-1R dimer formation in the presence of this heterodimeric receptor's ligand. However, it was clear that in both Y201 MSCs and Y201-derived adipocytes, a significant decrease in IR:IGF-1R hybrid count was seen upon stimulation of these cells with insulin relative to the unstimulated basal groups (Fig. 11A). This would indicate that IR:IGF-1R heterodimeric receptors are innately present on the cell surface and that the presence of insulin is not prerequisite for their dimerisation. Whether this is also applicable to homodimeric insulin receptors and IGF-1R is yet to be identified. Another finding of particular note from this quantitative analysis was the apparent difference in the insulin response between MSCs and adipocytes. Upon 5 minutes of insulin stimulation, the abundance of heterodimeric receptors drops significantly but with increasing duration of insulin stimulation, the levels of IR:IGF-1R hybrids recover until, at 20 minutes, they are no longer statistically different from the original value. Contrary to this, Y201-derived adipocytes see a greater drop in hybrid receptor count upon 5 minute stimulation but the abundance of these receptors does not recover, rather it continues to decrease drastically up to the 20 minute maximum duration of insulin stimulation.

The cause for this difference in response is undetermined but a proposed mechanism is as follows: it may be that, since IGF-1R is expressed only at a low level in terminally differentiated adipocytes (Fig. 8) and insulin has a much lower affinity for IGF-1R than it does for IR, the ligand-binding kinetics differ between IR:IGF-1R hybrids and dimeric IRs. This difference in binding affinity may mean that upon binding to either of these receptors to induce an intracellular signal, insulin occupies the ligand-binding site of the higher affinity IR homodimers more securely and takes longer to dissociate than it does when binding to the lower affinity receptor hybrids. As a result, monomeric insulin receptor

subunits would be occupied in homodimers for a greater period of time than the IGF-1R subunits would be in heterodimers and as time progresses, fewer free IR monomers are available so the ratio of free IGF-1R:IR monomer abundance increases. While this would mean a greater degree of IR signalling is observed in these cells, the lack of monomeric IR partners for monomeric IGF-1R subunits would result in the decrease in IR:IGF-1R hybrid abundance observed in the PLA. Whether this is a plausible mechanism for this finding remains to be verified; analysis of the heterodimeric receptor's affinity for insulin may be a suitable starting point for this purpose.

While this postulation may help to explain the gradual decrease in PLA signal with increasing duration of insulin stimulation in adipocytes, a separate idea must be proposed for the recovery pattern of IR:IGF-1R dimers observed in MSCs. The primary antibodies used for PLA are both specific to the intracellular region of the β subunit of each receptor monomer. This region harbours the tyrosine kinase domain responsible for transphosphorylation of the monomer's bound partner and is known to undergo a conformational change upon the binding of insulin to the extracellular ligand-binding domain (Ward, Menting and Lawrence, 2013; Maruyama, 2014). It is possible that this conformational change masks one or both epitopes targeted by the primary antibodies and, after fixing the cells, means the antibodies cannot effectively bind each monomer. This would result in a decrease in PLA signal despite the number of hybrid receptors remaining unchanged following insulin stimulation. Concerning the upward trend of PLA signal following the initial drop from 0 to 5 minutes of insulin stimulation, it may be that this conformational change takes between 10 and 20 minutes to be reversed, resetting the receptor and allowing subsequent activations by insulin after the 20 minute time point. This cyclical response would be exaggerated in the case of PLA as, due to serum starvation prior to PLA combined with the absence of insulin in cell culture media which would otherwise be present in human tissues, all cells used in this assay are synchronised and upon first stimulation with insulin, respond contemporaneously to produce the pattern perceived. Once again, this suggestion is speculation but may provide a starting point for understanding these differences in hybrid receptor abundance. It may be pertinent to perform PLA on cells stimulated with insulin for greater periods of time to see whether the receptor count levels out as the cells become desynchronised in their insulin response.

An additional result worth noting is the difference in the decrease in PLA signal in MSCs and adipocytes between 0 and 5 minutes of insulin stimulation (Fig. 11B). In the Y201 MSCs, a 1.3-fold decrease is observed in PLA signal in the initial drop following 5 minutes of insulin stimulation. In contrast, a 4.2-fold decrease is seen in Y201-derived adipocytes in the same period. This difference could be a result of the two previously hypothesised mechanisms working in combination; while the decrease in PLA signal in MSCs may be due to hindered antibody binding, the decrease in PLA signal in adipocytes may suggest a synergy between hindered antibody binding and sequestration of IR monomers in higher

affinity homodimers due to decreased IGF-1R expression, meaning that not only is the PLA signal reduced as a result of inaccessible epitopes, but also due to failure of IGF-1R monomers to find suitable IR partners for the formation of heterodimers. This would explain the greater decrease in PLA signal observed in Y201-derived adipocytes.

4.2.4 CRISPR-Cas9 knockout system may operate with low efficiency

The plan to investigate IR and IGF-1R functionally on an independent basis formed a major aim in this project. This required the generation of two cell lines, facilitated with the use of a CRISPR-Cas9 system to disrupt the genetic loci of *INSR* and *IGF-1R* and abolish their expression. Transfection of Y201 MSCs with the RFP-tagged *INSR*/*IGF-1R*-targeting CRISPR-Cas9 constructs was successful (Fig. 12) and allowed the expansion of around 20 colonies for each knockout. Unfortunately, due to low cell viability following transfection and sorting, and several instances of cell culture contamination of unidentifiable provenance, few colonies remained to screen via SDS-PAGE and western blotting to confirm whether each receptor had been successfully knocked out. The first screening revealed several candidates that appeared to express very low levels of each receptor (Fig. 13A) but the second screening showed significant levels of each receptor for these promising candidates (Fig. 13B). It is unusual to see such a range of expression intensity across these candidates as this method of CRISPR-Cas9-directed knockout should generally be either unsuccessful or successful, with the exception of heterozygous deletion, rather than slightly reducing receptor expression by varying degrees as though the genes had been knocked down.

Although faint bands still appear for the suspected knockouts, this could be caused by several unrelated factors. Firstly, the IR and IGF-1R proteins share a high degree of homology, estimated to be 50% similar overall and sharing up to 80% homology in the tyrosine kinase domain (Cai *et al.*, 2017). The antibodies used for western blot detection were specific to epitopes on the intracellular β subunits for each receptor, upon which the homologically-similar tyrosine kinase domain is located. This could suggest nonspecific binding of antibodies to the opposite receptor in the western blot leading to the formation of faint bands where a knockout may have been successful. The similar molecular weights of the β subunits further support this as a plausible idea, but cross-reactivity of these antibodies would likely have affected the negative controls of the PLA (Fig. 10) so this may not be the case. Moreover, the epitopes targeted by each antibody are not specified at their commercial source, making it impossible to identify whether the epitopes are partially conserved between receptors. An additional explanation could be the sensitivity of the chemiluminescent substrate used for the detection of protein bands. The substrate used for this purpose is highly sensitive and can detect picograms of protein; with this knowledge, it is possible that when loading SDS-PAGE gels, overspill of samples into adjacent wells deposited picograms of receptor proteins and led to the detection of faint

bands where there would otherwise have been none. Unfortunately, these factors meant that genuine receptor knockouts were not identified within the time frame available for this project, so the adipogenic potential of each receptor could not be determined. It would be beneficial to screen these candidates once again using an alternative method such as PCR and sequencing of the Cas9-targeted loci to determine whether any of the promising candidates are legitimate knockouts.

4.2.5 Double-tagged GLUT4 will enable future metabolic analysis

As a benefit to future work that successfully generates cell lines expressing each receptor in isolation, this investigation looked to generate a construct that could be used to visualise any changes in function in the absence of IR or IGF-1R. The HA-GLUT4-GFP construct to be used for this purpose required sgRNA targeting *SLC2A4* with a selectable marker. Plasmids fulfilling these criteria were successfully generated and validated with sequencing, individually targeting the 5' and 3' homology arms of *SLC2A4* and encoding either GFP, for visual confirmation of plasmid function and transfection, or PuroR, to be used in practice for antibiotic selection of successfully transfected cells. The GFP-tagged plasmids were tested via transfection and fluorescence microscopy (Fig. 14) which further confirmed plasmid function. PuroR-encoding plasmids were not experimentally tested in this way due to time constraints but optimisation of puromycin concentration will need to be performed to generate a kill curve for Y201 MSCs transfected with the 5' and 3' plasmids alongside the linear HA-GLUT4-GFP construct. The generation of this tool has made it possible to directly analyse the downstream effects of IR/IGF-1R knockout on insulin signalling, and future use of this technique will provide support for the results of the FRET data analysis, giving an additional indicator of altered insulin signalling capacity. Combining these two analyses will show not only the effect of receptor knockout on glucose uptake, but will provide a useful insight into the signalling that leads to glucose influx; if GLUT4 trafficking and glucose uptake are inextricably linked as expected, this would provide further evidence for the validity of FRET as method of determining changes in metabolic insulin signalling.

4.3 Project limitations

As is evident from the lack of success in generating and differentiating receptor knockouts, several unforeseeable obstacles were encountered in the course of this investigation that made certain results unachievable within the time frame available. Overall, one of the major issues faced in this project that affected the proceedings of all subsequent work stemmed from delays in the execution of successful transfection. While at the beginning of the project the plasmids required for HA-GLUT4-GFP expression and CRISPR-Cas9-directed *INSR*/*IGF-1R* knockout were generated and prepared

successfully, they were dependent on transfection to allow any further work to continue. Several months were spent troubleshooting transfection of these plasmids which were exhibiting no fluorescence in Y201 MSCs and were causing high levels of cell death. At this stage the project aims were modified to be achievable with the remaining time, giving rise to the PLA and FRET analyses which enabled additional contextually relevant and significant findings to be acquired. These transfection issues were eventually resolved and appeared to be arising from the plasmid preparation technique originally employed prior to transfection. Unfortunately the issues encountered led to heavy delays with remaining experimental work, especially regarding receptor knockout so compromises had to be made with respect to the original aims of the project.

Upon successful transfection of the RFP-tagged *INSR*/*IGF-1R*-targeted Cas9 plasmids, fluorescent cells were sorted and isolated via FACS and plated both as single cells and groups of cells of varying density. Despite the use of conditioned media for this plating, cell viability was incredibly low, especially for single cells. This resulted in the acquisition of very few knockout candidates using this method; as stated, only around 20 colonies were obtained. This number is very low compared to the number of RFP-positive cells that were sorted for clonal expansion as the majority of transfected cells were not viable after FACS. This high degree of cell death could be a result of off-target mutation induced by the Cas9 enzyme (Hsu *et al.*, 2013), reduced viability of cells lacking IR/IGF-1R, or cumulative cell stress following transfection and single-cell isolation in a short time frame. To isolate cells from the cultures plated at varying densities, each culture required expansion prior to serial dilution with the aim of achieving clonal colonies. Serial dilution of these cells was necessitated by the migratory nature of Y201 MSCs which made traditional single-cell isolation techniques impossible. Unfortunately this process required a number of months to achieve suitable colonies and the many intermediate steps for colony expansion led to contamination of cell cultures on multiple occasions, resulting in the loss of many knockout candidates. Ultimately, this reduced the final number of clonal colonies available for SDS-PAGE and western blot screening and reduced the chance of identifying cells that underwent successful Cas9 editing. These two aforementioned issues had a significant impact on downstream analysis; receptor knockouts were not successfully identified and the delays meant that even with success, it would not have been feasible to analyse the capacity of these cells to differentiate within the time frame of the project.

Moving on from the issues that hindered the execution of experimental work in this investigation, there are a number of analyses that would have complemented the presented findings well. It may have been possible to carry out this work in the absence of delays but this was ultimately not practicable in the time available. One result that would have augmented the validation of Y201 MSCs for use as a model to investigate adipogenesis would be more in-depth analysis of 3T3-L1 fibroblast differentiation.

Although this was indirectly measured with analysis of the FRET data, analysis of adipocyte marker expression and ORO staining in 3T3-L1 fibroblasts would have consolidated the findings presented and provided another comparison between the two cell lines. An additional limitation in this investigation regards the PLA analysis. The PLA results show changes in the proportion of IR:IGF-1R hybrid receptors following adipogenesis; the antibodies used are specific to the intracellular portion of the β subunit of the corresponding receptor which takes into account levels of IR-A:IGF-1R and IR-B:IGF-1R combined as the presence of exon 11 has no defined effect on the binding affinity of antibodies for the β subunit. No IR isoform-specific monoclonal antibodies were available for use during this investigation so whether the ratio of IR-A:IGF-1R to IR-B:IGF-1R hybrid receptors varies throughout the differentiation process was not an attainable result. This is something that would need to be considered in any future investigations looking to analyse IR isoforms independently.

4.4 Future work

4.4.1 Analysis of remaining insulin receptors

The present investigation has succeeded in obtaining novel information concerning the involvement of insulin receptors in adipogenesis and the use of Y201 MSCs as a model for adipogenesis-related disease states. There is, however, a significant amount of knowledge yet to be gained in this context. First and foremost, with insulin having a total of six major receptors, several of these were not directly investigated in this project which had the capacity to analyse only IGF-1R:IGF-1R, IGF-1R:IR, and IR:IR dimers; IR was used as an umbrella term in this investigation to encompass IR-A and IR-B which must be disconnected to get a true idea of the role of the six individual dimeric insulin receptors in the cellular processes they influence. One method to facilitate such an analysis would be to use sequential CRISPR-Cas9-directed knockout of both *INSR* and *IGF-1R* before ectopic expression of DNA encoding either IR-A, IR-B, or IGF-1R. This would generate three cell lines, each expressing a single one of these receptors, and would allow investigation of homodimeric receptors independently. In addition to this, the PLA used to identify IR:IGF-1R dimers could be expanded upon for future analysis; by obtaining antibodies specific to each isoform of IR, the changes in expression of each isoform, and abundance of IR heterodimers before and after Y201 MSC differentiation could be quantified and used to identify their potential roles in adipogenesis. These techniques would help to build a better picture of the role of individual receptors in adipogenesis and could also be a starting point for investigating hybrid receptor prevalence in the differentiation of other Y201 MSC lineages such as osteogenesis and chondrogenesis in which insulin receptors are known to play a role (Phornphutkul, Wu and Gruppuso, 2006; Ferron *et al.*, 2010; Zhang *et al.*, 2020).

4.4.2 Knockout validation and differentiation

With the generation of *INSR*$^{-/-}$ and *IGF-1R*$^{-/-}$ cell lines proving hard to achieve, it would be useful to screen candidates with additional methods. While promising candidates were identified in this investigation, a second screening with SDS-PAGE and western blotting made the results difficult to interpret, especially considering the possibility of protein bands appearing where there may have been none due to the discussed issues with detection. To remedy this, one method that could be used for additional validation of knockout success is the use of PCR amplification of the deletion site followed by agarose gel electrophoresis. Using PCR primers that encompass the site targeted by Cas9 would mean PCR does not produce an amplicon for successful knockouts which would be visible on an agarose gel. Other methods that could be used to check for expression of the targeted genes include RT-qPCR and northern blot analysis, both of which would determine the level of transcription of *INSR* or *IGF-1R* for each candidate. In the event that none of the candidates produced in the present investigation are found to have been successfully edited, the CRISPR-Cas9 system would need to be utilised once again on a larger scale to maximise the chance of isolating successfully edited cells.

4.4.3 Metabolic and mitogenic analysis

The aims of this project were designed to feed into the greater aim of delineating the overlapping pathways associated with insulin receptor signalling. While adipogenesis is a process heavily influenced by insulin receptor signalling, there are myriad other signalling pathways and cellular responses modulated by insulin. Chief among these are the metabolic pathway leading to GLUT4 translocation and glucose influx, and the mitogenic Ras/MAPK pathway leading to cell growth and proliferation. To greatly enhance our understanding of the influence of each insulin receptor on cell function, and to open avenues to explore the causes and potential therapeutic interventions for T2DM and insulin-associated cancers, these pathways must be investigated in the context of each of insulin's six receptors. Such an investigation could begin in a similar way to this project: by generating three cell lines, each expressing only one of the three receptor monomers, the activation of mitogenic and metabolic cell responses could be determined in the context of each receptor. For metabolic analysis, methods such as those presented in this investigation could be employed; the use of FRET and the HA-GLUT4-GFP construct would allow the metabolic response of each cell line to be identified and any differences between cell lines would indicate that the homodimeric receptors promote differential activation of downstream effects. For the analysis of the mitogenic response, cell proliferation assays and DNA content analysis would serve as a suitable method to determine activation of this process. To consolidate these findings, a phosphoproteomic analysis of the pathways activated downstream of each receptor upon stimulation with

insulin would confirm whether it is at the receptor level that these pathways diverge or whether there is deviation in the intracellular mechanisms associated with these receptors.

4.4.4 Clinical applications

Although the potential therapeutic use of insulin analogues to manage diseases associated with insulin signalling has not been experimentally covered in the present investigation, it is important to understand the current situation with regard to their function and administration. Five major insulin analogues are clinically available for the management of diabetes: short-acting lispro, aspart, and glulisine, and long-acting glargine and detemir. Insulin analogues are designed to deliver antihyperglycaemic effects in a more consistent manner following subcutaneous injection than exogenous insulin and can exhibit tissue selectivity for the targeted management of glucose homeostasis (Hennige *et al.*, 2006). Part of the reason for this tissue selectivity is the different binding affinities of IR isoforms and IGF-1R for each of these insulin analogues (Varewijck and Janssen, 2012), but their effects are not identical to insulin and in some cases can increase the risk of cancer as a result of IR/IGF-1R-mediated Ras/MAPK pathway activation (Stammberger, Seipke and Bartels, 2006; Sciacca *et al.*, 2010). Overall, the specific effects of each analogue on insulin signalling pathways as a result of preferential receptor binding are not well defined and studies investigating the risk of cancer in diabetic patients have not fully accounted for the influence of therapeutically-administered insulin analogues. This highlights the need for further investigation into the metabolic and mitogenic responses achieved upon stimulation of each receptor on an individual level and how they might be modulated with the use of insulin analogues. In a situation where some receptors are found to promote metabolic signalling and others promote mitogenic signalling or adipogenic signalling, the use of receptor-specific insulin analogues could be used to independently bring about or prevent these cellular responses. This could have implications for the treatment of disease states associated with each of these signalling pathways such as obesity, T2DM, and cancer.

It is also worth noting that, since insulin is known to have an effect on the lineage commitment of Y201 MSCs, especially with regard to adipogenic, osteogenic, and chondrogenic differentiation (Phornphutkul, Wu and Gruppuso, 2006; Ferron *et al.*, 2010; Zhang *et al.*, 2020), it would be beneficial to biomedical research to identify whether each of the receptors for insulin cause preferential activation or inhibition of the pathways involved with commitment to these lineages. In this case, it may be possible to selectively activate or inhibit these pathways to drive Y201 MSCs down a particular lineage which could prove useful for regenerative therapies. Apropos of regenerative medicine, any effect of each receptor on cell motility and secretion of intercellular signalling molecules should be determined to identify any possibility of enhancing the regenerative capacity of

Y201 MSCs by stimulating or inhibiting particular receptors with the use of receptor-specific insulin analogues.

4.5 Conclusions

Overall, this investigation revealed a range of novel insights into the function of insulin's numerous receptors and the capacity of Y201 MSCs to be used as a physiologically relevant alternative to 3T3-L1 cells in the context of human disease states. It has been shown that Y201 MSCs can be induced to differentiate into adipocytes with high success and that the physiological response of Y201-derived adipocytes is comparable to that of 3T3-L1-derived adipocytes. Although differences in this response were identified, it may point to variation in the metabolic signalling mechanisms between human and mouse cells. This may make Y201 MSCs more suitable for the investigation of human insulin signalling and adipogenesis. With regard to insulin receptor signalling, the changes in IR and IGF-1R protein expression throughout adipogenesis have been demonstrated and may reflect their primary roles in metabolic and mitogenic signalling respectively, especially due to the downregulation of IGF-1R in adipocytes which would be expected for a growth factor receptor. The presence of heterodimeric IR:IGF-1R hybrids was also characterised in Y201 MSCs and Y201-derived adipocytes using PLA and revealed distinct patterns of hybrid abundance when stimulated with insulin across a range of time points. Two mechanisms by which these patterns might emerge have been suggested but remain to be experimentally tested. In addition to this, with the aim of generating *INSR*$^{-/-}$ and *IGF-1R*$^{-/-}$ cell lines, CRISPR-Cas9 constructs were used for attempted deletion of these genes. While it is unclear whether any of the knockout candidates produced were successfully edited using this system, additional options for knockout validation have been discussed and could be explored further in future work. Finally, constructs have been generated to allow metabolic analysis of any valid receptor knockouts by expressing a double tagged HA-GLUT4-GFP protein that will allow the translocation of GLUT4 to be visualised in the context of each receptor to identify the effect they have on metabolic insulin signalling.

While some of the original aims of this experimental work were unsuccessful or unattainable in the project's time frame, the work presented has laid a strong foundation for the pursuit and continuation of this work in future. Future work may aim to generate cell lines expressing the three insulin receptor monomers independently in order to characterise homodimeric receptor signalling. This could use the HA-GLUT4-GFP construct for metabolic analysis and a phosphoproteomic approach would allow interrogation of the intracellular signalling pathways downstream of each of these receptors. Furthermore, a repeat of the PLA experiments using IR isoform-specific antibodies would help to elucidate the function of each insulin receptor in adipogenesis as well as in the differentiation of MSCs via alternative lineages. Finally, it could be clinically

significant to determine the potential to preferentially stimulate or inhibit certain pathways downstream of insulin receptors with the use of receptor-specific insulin analogues. By modulating these pathways independently of one another, therapeutic intervention such as the treatment of diabetes and obesity without promoting the development of cancer, inhibiting cell proliferation in cancers without altering glucose homeostasis, and enhancing cell proliferation, motility, or secretion for regenerative therapies could be achievable. This would have a significant impact on the treatment of many human disease states and highlights the importance of elucidating the role of each of insulin's six receptors in the cellular mechanisms and downstream pathways they influence.

List of abbreviations

ANOVA	Analysis of variance
BMSC	Bone-marrow-derived mesenchymal stem cell
BSA	Bovine serum albumin
BSA/GLY/SAP	Bovine serum albumin/glycine/saponin
C/EBPα	CCAAT/enhancer-binding protein alpha
CFP	Cyan fluorescent protein
CR	Cysteine-rich domain
CRISPR	Clustered regularly interspaced short palindromic repeats
DALY	Disability-adjusted life year
DAPI	4'6-diamidino-2-phenylindole
ddH_2O	Double-distilled H_2O
DMEM	Dulbecco's modified eagle medium
DMSO	Dimethyl sulphoxide
DNA	Deoxyribonucleic acid
DSB	Double-strand break
EDTA	Ethylenediaminetetraacetic acid
FABP4	Fatty acid binding protein 4
FACS	Fluorescence-activated cell sorting
FBS	Foetal bovine serum
Fn-III	Fibronectin type III domain
FRET	Förster resonance energy transfer
GAP	GTPase-activating protein
GAPDH	Glyceraldehyde 3-phosphate dehydrogenase
GEF	Guanine nucleotide exchange factor
GFP	Green fluorescent protein
GLUT4	Glucose transporter type 4
HA	Haemagglutinin
HDR	Homology-directed repair
hTERT	Human telomerase reverse transcriptase
IBMX	3-isobutyl-1-methylxanthine
IGF-1	Insulin-like growth factor 1
IGF-2	Insulin-like growth factor 2
IGF-1R	Insulin-like growth factor 1 receptor
IGF-1R	Insulin-like growth factor 1 receptor (gene)
INSR	Insulin receptor (gene)
IR	Insulin receptor
IR-A	Insulin receptor isoform A
IR-B	Insulin receptor isoform B

IRS-1	Insulin receptor substrate 1
L1/L2	Leucine-rich repeat domain 1/2
LB	Lysogeny broth
LN_2	Liquid nitrogen
mAb	Monoclonal antibody
MAPK	Mitogen-activated protein kinase
MSC	Mesenchymal stem cell
mTORC1	Mammalian target of rapamycin complex 1
NEFA	Non-esterified fatty acid
NHEJ	Non-homologous end joining
ORO	Oil red O
PBS	Phosphate-buffered saline
PDBe	Protein data bank in Europe
PFA	Paraformaldehyde
PI3K	Phosphatidylinositol-3-kinase
PLA	Proximity ligation assay
PPAR-γ	Peroxisome proliferator-activated receptor gamma
RFP	Red fluorescent protein
RTK	Receptor tyrosine kinase
SDS-PAGE	Sodium dodecyl-sulphate polyacrylamide gel electrophoresis
SEM	Standard error of the mean
sgRNA	Single guide ribonucleic acid
SHC1	SHC-transforming protein 1
SLC2A4	Solute carrier family 2 member 4
SNP	Single nucleotide polymorphism
SREBP-1c	Sterol regulatory element-binding transcription factor 1c
T1DM	Type 1 diabetes mellitus
T2DM	Type 2 diabetes mellitus
TBST	Tris-buffered saline with Tween20
YFP	Yellow fluorescent protein

Bibliography

Agha-Hosseini, F. *et al.* (2010) 'In vitro isolation of stem cells derived from human dental pulp', *Clinical transplantation*, 24(2), pp. E23–8.

Ali, A.T. *et al.* (2013) 'Adipocyte and adipogenesis', *European journal of cell biology*, 92(6-7), pp. 229–236.

Ali, O. (2013) 'Genetics of type 2 diabetes', *World journal of diabetes*, 4(4), pp. 114–123.

Bailyes, E.M. *et al.* (1997) 'Insulin receptor/IGF-I receptor hybrids are widely distributed in mammalian tissues: quantification of individual receptor species by selective immunoprecipitation and immunoblotting', *Biochemical Journal*, 327 (Pt 1), pp. 209–215.

Barnes, J.A. *et al.* (2020) 'Epidemiology and Risk of Amputation in Patients With Diabetes Mellitus and Peripheral Artery Disease', *Arteriosclerosis, thrombosis, and vascular biology*, 40(8), pp. 1808–1817.

Belfiore, A. *et al.* (2017) 'Insulin Receptor Isoforms in Physiology and Disease: An Updated View', *Endocrine reviews*, 38(5), pp. 379–431.

BioRender (no date). Available at: https://biorender.com/ (Accessed: 8 February 2021).

Brillon, D.J. *et al.* (1988) 'Functional and structural differences in human and rat-derived insulin receptors: characterization of the beta-subunit kinase activity', *Endocrinology*, 123(4), pp. 1837–1847.

Cai, W. *et al.* (2017) 'Domain-dependent effects of insulin and IGF-1 receptors on signalling and gene expression', *Nature communications*, 8, p. 14892.

Cao, J. *et al.* (2021) 'Developing standards to support the clinical translation of stem cells', *Stem cells translational medicine*, 10 Suppl 2, pp. S85–S95.

Carr, L.K. *et al.* (2008) '1-year follow-up of autologous muscle-derived stem cell injection pilot study to treat stress urinary incontinence', *International urogynecology journal and pelvic floor dysfunction*, 19(6), pp. 881–883.

Castell-Auví, A. *et al.* (2012) 'The effects of a cafeteria diet on insulin production and clearance in rats', *The British journal of nutrition*, 108(7), pp. 1155–1162.

Cell Signaling Technology (2003) *Insulin Receptor Signaling*, *Cell Signaling Technology*. Available at: https://www.cellsignal.co.uk/pathways/insulin-receptor-signaling-pathway (Accessed: 7 June 2022).

Chakrabarti, P. *et al.* (2013) 'Insulin inhibits lipolysis in adipocytes via the evolutionarily conserved mTORC1-Egr1-ATGL-mediated pathway', *Molecular and cellular biology*, 33(18), pp. 3659–3666.

Charron, M.J. *et al.* (1989) 'A glucose transport protein expressed predominately in insulin-responsive tissues', *Proceedings of the National Academy of Sciences of the United States of America*, 86(8), pp. 2535–2539.

Cheatham, B. and Kahn, C.R. (1992) 'Cysteine 647 in the insulin receptor is required for normal covalent interaction between alpha- and beta-subunits and signal transduction', *The Journal of biological chemistry*, 267(10), pp. 7108–7115.

Chu, D.-T. *et al.* (2014) ‘Expression of adipocyte biomarkers in a primary cell culture models reflects preweaning adipobiology’, *The Journal of biological chemistry*, 289(26), pp. 18478–18488.

Cignarelli, A. *et al.* (2019) ‘Insulin and Insulin Receptors in Adipose Tissue Development’, *International journal of molecular sciences*, 20(3). Available at: https://doi.org/10.3390/ijms20030759.

Costa, L.A. *et al.* (2021) ‘Functional heterogeneity of mesenchymal stem cells from natural niches to culture conditions: implications for further clinical uses’, *Cellular and molecular life sciences: CMLS*, 78(2), pp. 447–467.

Cusi, K. *et al.* (2000) ‘Insulin resistance differentially affects the PI 3-kinase- and MAP kinase-mediated signaling in human muscle’, *The Journal of clinical investigation*, 105(3), pp. 311–320.

Dif, N. *et al.* (2006) ‘Insulin activates human sterol-regulatory-element-binding protein-1c (SREBP-1c) promoter through SRE motifs’, *Biochemical Journal*, 400(1), pp. 179–188.

Dubuc, P.U. (1976) ‘The development of obesity, hyperinsulinemia, and hyperglycemia in ob/ob mice’, *Metabolism: clinical and experimental*, 25(12), pp. 1567–1574.

Ferron, M. *et al.* (2010) ‘Insulin Signaling in Osteoblasts Integrates Bone Remodeling and Energy Metabolism’, *Cell*, 142(2), pp. 296–308.

Foretz, M. *et al.* (1999) ‘Sterol regulatory element binding protein-1c is a major mediator of insulin action on the hepatic expression of glucokinase and lipogenesis-related genes’, *Proceedings of the National Academy of Sciences of the United States of America*, 96(22), pp. 12737–12742.

Franke, W.W., Hergt, M. and Grund, C. (1987) ‘Rearrangement of the vimentin cytoskeleton during adipose conversion: formation of an intermediate filament cage around lipid globules’, *Cell*, 49(1), pp. 131–141.

Frasca, F. *et al.* (1999) ‘Insulin receptor isoform A, a newly recognized, high-affinity insulin-like growth factor II receptor in fetal and cancer cells’, *Molecular and cellular biology*, 19(5), pp. 3278–3288.

Friedenstein, A.J., Chailakhjan, R.K. and Lalykina, K.S. (1970) ‘The development of fibroblast colonies in monolayer cultures of guinea-pig bone marrow and spleen cells’, *Cell and tissue kinetics*, 3(4), pp. 393–403.

Fulzele, K. *et al.* (2010) ‘Insulin receptor signaling in osteoblasts regulates postnatal bone acquisition and body composition’, *Cell*, 142(2), pp. 309–319.

Furuhashi, M. *et al.* (2014) ‘Fatty Acid-Binding Protein 4 (FABP4): Pathophysiological Insights and Potent Clinical Biomarker of Metabolic and Cardiovascular Diseases’, *Clinical Medicine Insights. Cardiology*, 8(Suppl 3), pp. 23–33.

Giorgino, F. *et al.* (1991) ‘Overexpression of insulin receptors in fibroblast and ovary cells induces a ligand-mediated transformed phenotype’, *Molecular endocrinology* , 5(3), pp. 452–459.

Goalstone, M. *et al.* (1997) ‘Insulin stimulates the phosphorylation and activity of farnesyltransferase via the Ras-mitogen-activated protein kinase pathway’, *Endocrinology*, 138(12), pp. 5119–5124.

Groop, L.C. *et al.* (1991) 'The role of free fatty acid metabolism in the pathogenesis of insulin resistance in obesity and noninsulin-dependent diabetes mellitus', *The Journal of clinical endocrinology and metabolism*, 72(1), pp. 96–107.

Gupta, M.K. *et al.* (2018) 'Insulin receptor-mediated signaling regulates pluripotency markers and lineage differentiation', *Molecular metabolism*, 18, pp. 153–163.

Gustafson, T.A. *et al.* (1995) 'Phosphotyrosine-dependent interaction of SHC and insulin receptor substrate 1 with the NPEY motif of the insulin receptor via a novel non-SH2 domain', *Molecular and cellular biology*, 15(5), pp. 2500–2508.

Haluska, P. *et al.* (2006) 'In vitro and in vivo antitumor effects of the dual insulin-like growth factor-I/insulin receptor inhibitor, BMS-554417', *Cancer research*, 66(1), pp. 362–371.

Hansen, B.F. *et al.* (1996) 'Sustained signalling from the insulin receptor after stimulation with insulin analogues exhibiting increased mitogenic potency', *Biochemical Journal*, 315 (Pt 1), pp. 271–279.

Hausman, D.B. *et al.* (2001) 'The biology of white adipocyte proliferation', *Obesity reviews: an official journal of the International Association for the Study of Obesity*, 2(4), pp. 239–254.

Havrankova, J., Roth, J. and Brownstein, M. (1978) 'Insulin receptors are widely distributed in the central nervous system of the rat', *Nature*, 272(5656), pp. 827–829.

Hennige, A.M. *et al.* (2006) 'Tissue selectivity of insulin detemir action in vivo', *Diabetologia*, 49(6), pp. 1274–1282.

Heuson, J.C. and Legros, N. (1972) 'Influence of insulin deprivation on growth of the 7,12-dimethylbenz(a)anthracene-induced mammary carcinoma in rats subjected to alloxan diabetes and food restriction', *Cancer research*, 32(2), pp. 226–232.

Hillier, T.A. and Pedula, K.L. (2003) 'Complications in young adults with early-onset type 2 diabetes: losing the relative protection of youth', *Diabetes care*, 26(11), pp. 2999–3005.

Hoexter, D.L. (2002) 'Bone regeneration graft materials', *The Journal of oral implantology*, 28(6), pp. 290–294.

Hsu, P.D. *et al.* (2013) 'DNA targeting specificity of RNA-guided Cas9 nucleases', *Nature biotechnology*, 31(9), pp. 827–832.

Jaldin-Fincati, J.R. *et al.* (2017) 'Update on GLUT4 Vesicle Traffic: A Cornerstone of Insulin Action', *Trends in endocrinology and metabolism: TEM*, 28(8), pp. 597–611.

James, S. *et al.* (2015) 'Multiparameter Analysis of Human Bone Marrow Stromal Cells Identifies Distinct Immunomodulatory and Differentiation-Competent Subtypes', *Stem cell reports*, 4(6), pp. 1004–1015.

Johnston, L.W. *et al.* (2018) 'Association of NEFA composition with insulin sensitivity and beta cell function in the Prospective Metabolism and Islet Cell Evaluation (PROMISE) cohort', *Diabetologia*, 61(4), pp. 821–830.

Jørgensen, H. *et al.* (1994) 'Stroke in patients with diabetes. The Copenhagen Stroke Study', *Stroke; a journal of cerebral circulation*, 25(10), pp. 1977–1984.

Kabat, G.C. *et al.* (2009) 'Repeated measures of serum glucose and insulin in relation to

postmenopausal breast cancer', *International journal of cancer. Journal international du cancer*, 125(11), pp. 2704–2710.

Kasuga, M. *et al.* (1982) 'The structure of insulin receptor and its subunits. Evidence for multiple nonreduced forms and a 210,000 possible proreceptor', *The Journal of biological chemistry*, 257(17), pp. 10392–10399.

Khan, S. *et al.* (2021) 'Patterns and risk factors associated with index Lower Extremity Amputations (LEA) among Type 2 Diabetes Mellitus (T2DM) patients in Fiji', *Primary care diabetes*, 15(6), pp. 1012–1018.

Kilvert, A. and Fox, C. (2020) 'Hyperinsulinaemia and cancer risk: cause and effect?', *Practical diabetes*, 37(6), p. 223.

Kim, S.H. and Reaven, G.M. (2008) 'Insulin resistance and hyperinsulinemia: you can't have one without the other', *Diabetes care*, 31(7), pp. 1433–1438.

Klemm, D.J. *et al.* (2001) 'Insulin-induced adipocyte differentiation. Activation of CREB rescues adipogenesis from the arrest caused by inhibition of prenylation', *The Journal of biological chemistry*, 276(30), pp. 28430–28435.

Kolf, C.M., Cho, E. and Tuan, R.S. (2007) 'Mesenchymal stromal cells. Biology of adult mesenchymal stem cells: regulation of niche, self-renewal and differentiation', *Arthritis research & therapy*, 9(1), p. 204.

Kottaisamy, C.P.D. *et al.* (2021) 'Experimental animal models for diabetes and its related complications-a review', *Laboratory animal research*, 37(1), p. 23.

Kraus, N.A. *et al.* (2016) 'Quantitative assessment of adipocyte differentiation in cell culture', *Adipocyte*, 5(4), pp. 351–358.

Krüger, M. *et al.* (2008) 'Dissection of the insulin signaling pathway via quantitative phosphoproteomics', *Proceedings of the National Academy of Sciences of the United States of America*, 105(7), pp. 2451–2456.

Larsson, S.C., Orsini, N. and Wolk, A. (2005) 'Diabetes mellitus and risk of colorectal cancer: a meta-analysis', *Journal of the National Cancer Institute*, 97(22), pp. 1679–1687.

Lefterova, M.I. and Lazar, M.A. (2009) 'New developments in adipogenesis', *Trends in endocrinology and metabolism: TEM*, 20(3), pp. 107–114.

Leppänen, V.-M. *et al.* (2010) 'Structural determinants of growth factor binding and specificity by VEGF receptor 2', *Proceedings of the National Academy of Sciences of the United States of America*, 107(6), pp. 2425–2430.

Lin, X. *et al.* (2020) 'Global, regional, and national burden and trend of diabetes in 195 countries and territories: an analysis from 1990 to 2025', *Scientific reports*, 10(1), p. 14790.

Liu, H. *et al.* (2007) 'Structural basis for stem cell factor-KIT signaling and activation of class III receptor tyrosine kinases', *The EMBO journal*, 26(3), pp. 891–901.

Lobstein, T., Brinsden, H. and Neveux, M. (2022) *World Obesity Atlas 2022*. Available at: https://www.worldobesityday.org/assets/downloads/World_Obesity_Atlas_2022_WEB.pdf.

Lord, G.M. (2006) 'Leptin as a proinflammatory cytokine', *Contributions to nephrology*, 151, pp. 151–164.

Maruyama, I.N. (2014) ‘Mechanisms of activation of receptor tyrosine kinases: monomers or dimers’, *Cells* , 3(2), pp. 304–330.

Matulewicz, N. *et al.* (2017) ‘Markers of Adipogenesis, but Not Inflammation, in Adipose Tissue Are Independently Related to Insulin Sensitivity’, *The Journal of clinical endocrinology and metabolism*, 102(8), pp. 3040–3049.

Ma, X. *et al.* (2018) ‘Deciphering the Roles of PPARγ in Adipocytes via Dynamic Change of Transcription Complex’, *Frontiers in endocrinology*, 9, p. 473.

Monami, M. *et al.* (2009) ‘Sulphonylureas and cancer: a case-control study’, *Acta diabetologica*, 46(4), pp. 279–284.

Morcavallo, A. *et al.* (2011) ‘Research resource: New and diverse substrates for the insulin receptor isoform A revealed by quantitative proteomics after stimulation with IGF-II or insulin’, *Molecular endocrinology* , 25(8), pp. 1456–1468.

Morrione, A. and Belfiore, A. (2022) ‘Obesity, Diabetes, and Cancer: The Role of the Insulin/IGF Axis; Mechanisms and Clinical Implications’, *Biomolecules*, 12(5), p. 612.

Mosthaf, L. *et al.* (1990) ‘Functionally distinct insulin receptors generated by tissue-specific alternative splicing’, *The EMBO journal*, 9(8), pp. 2409–2413.

Mueckler, M. and Thorens, B. (2013) ‘The SLC2 (GLUT) family of membrane transporters’, *Molecular aspects of medicine*, 34(2-3), pp. 121–138.

Murphy, J.M. *et al.* (2003) ‘Stem cell therapy in a caprine model of osteoarthritis’, *Arthritis and rheumatism*, 48(12), pp. 3464–3474.

Murphy, M.B., Moncivais, K. and Caplan, A.I. (2013) ‘Mesenchymal stem cells: environmentally responsive therapeutics for regenerative medicine’, *Experimental & molecular medicine*, 45, p. e54.

New England Biolabs (2018) *High Efficiency Transformation Protocol using NEB 10-beta Competent E. coli (C3019I)*, *protocols.io*. Available at: https://doi.org/10.17504/protocols.io.nkvdcw6.

Okamoto, R. *et al.* (2020) ‘Organoid-based regenerative medicine for inflammatory bowel disease’, *Regenerative therapy*, 13, pp. 1–6.

Olzmann, J.A. and Carvalho, P. (2019) ‘Dynamics and functions of lipid droplets’, *Nature reviews. Molecular cell biology*, 20(3), pp. 137–155.

Orozco, L.J. *et al.* (2008) ‘Exercise or exercise and diet for preventing type 2 diabetes mellitus’, *Cochrane database of systematic reviews* , (3), p. CD003054.

Pandini, G. *et al.* (2002) ‘Insulin/insulin-like growth factor I hybrid receptors have different biological characteristics depending on the insulin receptor isoform involved’, *The Journal of biological chemistry*, 277(42), pp. 39684–39695.

Papa, V. *et al.* (1990) ‘Elevated insulin receptor content in human breast cancer’, *The Journal of clinical investigation*, 86(5), pp. 1503–1510.

Patel, A.N. *et al.* (2008) ‘Multipotent menstrual blood stromal stem cells: isolation, characterization, and differentiation’, *Cell transplantation*, 17(3), pp. 303–311.

Phornphutkul, C., Wu, K.-Y. and Gruppuso, P.A. (2006) ‘The role of insulin in

chondrogenesis', *Molecular and cellular endocrinology*, 249(1-2), pp. 107–115.

Pierre-Eugene, C. *et al.* (2012) 'Effect of insulin analogues on insulin/IGF1 hybrid receptors: increased activation by glargine but not by its metabolites M1 and M2', *PloS one*, 7(7), p. e41992.

Pisani, P. (2008) 'Hyper-insulinaemia and cancer, meta-analyses of epidemiological studies', *Archives of physiology and biochemistry*, 114(1), pp. 63–70.

Pittenger, M.F. *et al.* (1999) 'Multilineage potential of adult human mesenchymal stem cells', *Science*, 284(5411), pp. 143–147.

Prestwich, T.C. and Macdougald, O.A. (2007) 'Wnt/beta-catenin signaling in adipogenesis and metabolism', *Current opinion in cell biology*, 19(6), pp. 612–617.

Prockop, D.J. (2007) '"Stemness" does not explain the repair of many tissues by mesenchymal stem/multipotent stromal cells (MSCs)', *Clinical pharmacology and therapeutics*, 82(3), pp. 241–243.

Rajapaksha, H. and Forbes, B.E. (2015) 'Ligand-Binding Affinity at the Insulin Receptor Isoform-A and Subsequent IR-A Tyrosine Phosphorylation Kinetics are Important Determinants of Mitogenic Biological Outcomes', *Frontiers in endocrinology*, 6, p. 107.

Ran, F.A. *et al.* (2013) 'Genome engineering using the CRISPR-Cas9 system', *Nature protocols*, 8(11), pp. 2281–2308.

Robert, A.W. *et al.* (2020) 'Adipogenesis, Osteogenesis, and Chondrogenesis of Human Mesenchymal Stem/Stromal Cells: A Comparative Transcriptome Approach', *Frontiers in cell and developmental biology*, 8, p. 561.

Roden, M. *et al.* (1996) 'Mechanism of free fatty acid-induced insulin resistance in humans', *The Journal of clinical investigation*, 97(12), pp. 2859–2865.

Rodríguez-Vázquez, M. *et al.* (2015) 'Chitosan and Its Potential Use as a Scaffold for Tissue Engineering in Regenerative Medicine', *BioMed research international*, 2015, p. 821279.

Rorsman, P. and Renström, E. (2003) 'Insulin granule dynamics in pancreatic beta cells', *Diabetologia*, 46(8), pp. 1029–1045.

Rosen, E.D. *et al.* (2002) 'C/EBPα induces adipogenesis through PPARγ: a unified pathway', *Genes & development*, 16(1), pp. 22–26.

Rose, P.P. *et al.* (2007) 'The insulin receptor is essential for virus-induced tumorigenesis of Kaposi's sarcoma', *Oncogene*, 26(14), pp. 1995–2005.

Salanti, G. *et al.* (2009) 'Underlying genetic models of inheritance in established type 2 diabetes associations', *American journal of epidemiology*, 170(5), pp. 537–545.

Savkur, R.S., Philips, A.V. and Cooper, T.A. (2001) 'Aberrant regulation of insulin receptor alternative splicing is associated with insulin resistance in myotonic dystrophy', *Nature genetics*, 29(1), pp. 40–47.

Scapin, G. *et al.* (2018) 'Insulin Receptor ectodomain in complex with one insulin molecule'. Worldwide Protein Data Bank. Available at: https://doi.org/10.2210/pdb6ce7/pdb.

Scherer, P.E. (2006) ‘Adipose tissue: from lipid storage compartment to endocrine organ’, *Diabetes*, 55(6), pp. 1537–1545.

Schlessinger, J. (2000) ‘Cell signaling by receptor tyrosine kinases’, *Cell*, 103(2), pp. 211–225.

Sciacca, L. *et al.* (2010) ‘Insulin analogues differently activate insulin receptor isoforms and post-receptor signalling’, *Diabetologia*, 53(8), pp. 1743–1753.

Serrano, R. *et al.* (2005) ‘Differential gene expression of insulin receptor isoforms A and B and insulin receptor substrates 1, 2 and 3 in rat tissues: modulation by aging and differentiation in rat adipose tissue’, *Journal of molecular endocrinology*, 34(1), pp. 153–161.

Shepherd, P.R., Withers, D.J. and Siddle, K. (1998) ‘Phosphoinositide 3-kinase: the key switch mechanism in insulin signalling’, *Biochemical Journal*, 333 (Pt 3), pp. 471–490.

Shigematsu, S. *et al.* (2003) ‘The adipocyte plasma membrane caveolin functional/structural organization is necessary for the efficient endocytosis of GLUT4’, *The Journal of biological chemistry*, 278(12), pp. 10683–10690.

Silbernagel, G. *et al.* (2011) ‘Effects of 4-week very-high-fructose/glucose diets on insulin sensitivity, visceral fat and intrahepatic lipids: an exploratory trial’, *The British journal of nutrition*, 106(1), pp. 79–86.

Smith, B.J. *et al.* (2010) ‘Structural resolution of a tandem hormone-binding element in the insulin receptor and its implications for design of peptide agonists’, *Proceedings of the National Academy of Sciences of the United States of America*, 107(15), pp. 6771–6776.

Staiger, H. *et al.* (2009) ‘Pathomechanisms of type 2 diabetes genes’, *Endocrine reviews*, 30(6), pp. 557–585.

Stammberger, I., Seipke, G. and Bartels, T. (2006) ‘Insulin glulisine--a comprehensive preclinical evaluation’, *International journal of toxicology*, 25(1), pp. 25–33.

Stenkula, K.G. and Erlanson-Albertsson, C. (2018) ‘Adipose cell size: importance in health and disease’, *American journal of physiology. Regulatory, integrative and comparative physiology*, 315(2), pp. R284–R295.

Stirling, D.R. *et al.* (2021) ‘CellProfiler 4: improvements in speed, utility and usability’, *BMC bioinformatics*, 22(1), p. 433.

Sugihara, H. *et al.* (1987) ‘Proliferation of unilocular fat cells in the primary culture’, *Journal of lipid research*, 28(9), pp. 1038–1045.

Sun, X.J. *et al.* (1991) ‘Structure of the insulin receptor substrate IRS-1 defines a unique signal transduction protein’, *Nature*, 352(6330), pp. 73–77.

Tanti, J.-F. *et al.* (2001) ‘Assays of Glucose Entry, Glucose Transporter Amount, and Translocation’, in G. Ailhaud (ed.) *Adipose Tissue Protocols*. Totowa, NJ: Springer New York, pp. 157–165.

Tatsumi, K. *et al.* (2013) ‘Tissue factor triggers procoagulation in transplanted mesenchymal stem cells leading to thromboembolism’, *Biochemical and biophysical research communications*, 431(2), pp. 203–209.

Teng, C.-F., Jeng, L.-B. and Shyu, W.-C. (2018) ‘Role of Insulin-like Growth Factor 1

Receptor Signaling in Stem Cell Stemness and Therapeutic Efficacy', *Cell transplantation*, 27(9), pp. 1313–1319.

Tokarz, V.L., MacDonald, P.E. and Klip, A. (2018) 'The cell biology of systemic insulin function', *The Journal of cell biology*, 217(7), pp. 2273–2289.

Tran, T.T., Medline, A. and Bruce, W.R. (1996) 'Insulin promotion of colon tumors in rats', *Cancer epidemiology, biomarkers & prevention: a publication of the American Association for Cancer Research, cosponsored by the American Society of Preventive Oncology*, 5(12), pp. 1013–1015.

Trautner, C. *et al.* (1997) 'Incidence of blindness in relation to diabetes. A population-based study', *Diabetes care*, 20(7), pp. 1147–1153.

Ullah, I., Subbarao, R.B. and Rho, G.J. (2015) 'Human mesenchymal stem cells - current trends and future prospective', *Bioscience reports*, 35(2). Available at: https://doi.org/10.1042/BSR20150025.

Varewijck, A.J. and Janssen, J.A.M.J.L. (2012) 'Insulin and its analogues and their affinities for the IGF1 receptor', *Endocrine-related cancer*, 19(5), pp. F63–75.

Verma, S. and Hussain, M.E. (2017) 'Obesity and diabetes: An update', *Diabetes & metabolic syndrome*, 11(1), pp. 73–79.

Versteyhe, S. *et al.* (2013) 'IGF-I, IGF-II, and Insulin Stimulate Different Gene Expression Responses through Binding to the IGF-I Receptor', *Frontiers in endocrinology*, 4, p. 98.

Wang, L. *et al.* (2017) 'Association between diabetes mellitus and subsequent ovarian cancer in women: A systematic review and meta-analysis of cohort studies', *Medicine*, 96(16), p. e6396.

Wang, Y. *et al.* (2012) 'Insulin promotes proliferation, survival, and invasion in endometrial carcinoma by activating the MEK/ERK pathway', *Cancer letters*, 322(2), pp. 223–231.

Ward, C.W., Menting, J.G. and Lawrence, M.C. (2013) 'The insulin receptor changes conformation in unforeseen ways on ligand binding: sharpening the picture of insulin receptor activation', *BioEssays: news and reviews in molecular, cellular and developmental biology*, 35(11), pp. 945–54, doi/10.1002/bies.201370111.

Werner, H., Sarfstein, R. and Laron, Z. (2021) 'The Role of Nuclear Insulin and IGF1 Receptors in Metabolism and Cancer', *Biomolecules*, 11(4). Available at: https://doi.org/10.3390/biom11040531.

White, M.F. *et al.* (1988) 'A cascade of tyrosine autophosphorylation in the beta-subunit activates the phosphotransferase of the insulin receptor', *The Journal of biological chemistry*, 263(6), pp. 2969–2980.

Wickham, H. *et al.* (2019) 'Welcome to the tidyverse', *Journal of open source software*, 4(43), p. 1686.

Wickham, H. and Bryan, J. (2022) *readxl: Read excel files (.xls and .xlsx) into R*. Github. Available at: https://github.com/tidyverse/readxl (Accessed: 6 September 2022).

Wollman, A.J.M. *et al.* (2022) 'Large scale, single-cell FRET-based glucose uptake measurements within heterogeneous populations', *iScience*, 25(4), p. 104023.

World Health Organization (2021a) *Diabetes*. Available at:

https://www.who.int/news-room/fact-sheets/detail/diabetes (Accessed: 15 December 2021).

World Health Organization (2021b) *Obesity and overweight*. Available at: https://www.who.int/news-room/fact-sheets/detail/obesity-and-overweight (Accessed: 13 May 2022).

Wu, S. *et al.* (2012) 'Reproductive tissues maintain insulin sensitivity in diet-induced obesity', *Diabetes*, 61(1), pp. 114–123.

Xu, J. *et al.* (2006) 'Insulin Enhances Growth Hormone Induction of the MEK/ERK Signaling Pathway *', *The Journal of biological chemistry*, 281(2), pp. 982–992.

Zhang, A.M.Y. *et al.* (2019) 'Endogenous Hyperinsulinemia Contributes to Pancreatic Cancer Development', *Cell metabolism*, 30(3), pp. 403–404.

Zhang, P. *et al.* (2020) 'Insulin impedes osteogenesis of BMSCs by inhibiting autophagy and promoting premature senescence via the TGF-β1 pathway', *Aging (Albany* [Preprint]. Available at: https://www.ncbi.nlm.nih.gov/pmc/articles/pmc7041775/.

Zhang, Q. *et al.* (2019) 'The post-PAM interaction of RNA-guided spCas9 with DNA dictates its target binding and dissociation', *Science advances*, 5(11), p. eaaw9807.

Zhou, Y.P. and Grill, V.E. (1994) 'Long-term exposure of rat pancreatic islets to fatty acids inhibits glucose-induced insulin secretion and biosynthesis through a glucose fatty acid cycle', *The Journal of clinical investigation*, 93(2), pp. 870–876.

Ziegler, A.N. *et al.* (2014) 'Insulin-like growth factor-II (IGF-II) and IGF-II analogs with enhanced insulin receptor-a binding affinity promote neural stem cell expansion', *The Journal of biological chemistry*, 289(8), pp. 4626–4633.

Zou, C., Wang, Y. and Shen, Z. (2005) '2-NBDG as a fluorescent indicator for direct glucose uptake measurement', *Journal of biochemical and biophysical methods*, 64(3), pp. 207–215.

Zuk, P.A. *et al.* (2001) 'Multilineage cells from human adipose tissue: implications for cell-based therapies', *Tissue engineering*, 7(2), pp. 211–228.